

AD-A032 448

ARIZONA UNIV TUCSON  
ON SPECTROSCOPIC MODELING OF THE WATER MOLECULE.(U)  
SEP 76 D ROGOVIN, H TIGELAAR

F/G 7/4

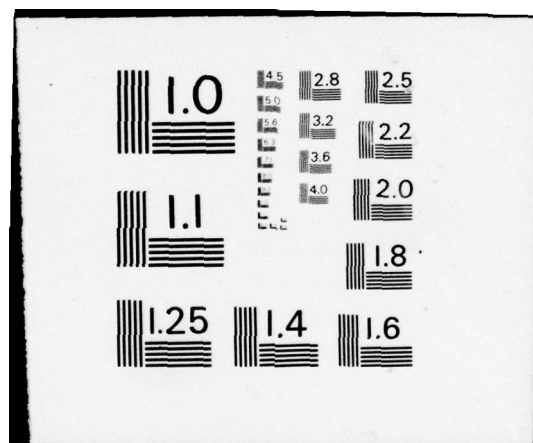
UNCLASSIFIED

AFWL-TR-75-84

F29601-74-A-0023  
NL

1 OF 1  
ADA032448





AFWL-TR-75-84

AFWL-TR-  
75-84

AD A032448

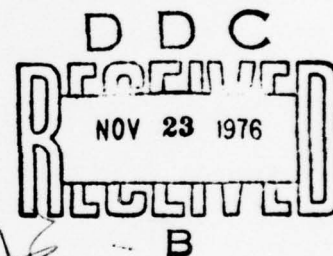


## ON SPECTROSCOPIC MODELING OF THE WATER MOLECULE

University of Arizona  
Tucson, Arizona 85721

September 1976

Final Report



Approved for public release; distribution unlimited.


AIR FORCE WEAPONS LABORAORY  
Air Force Systems Command  
Kirtland Air Force Base, NM 87117

This final report was prepared by the University of Arizona, Tucson, Arizona, under Contract F29601-74A-0023-0002, Job Order 33260913 with the Air Force Weapons Laboratory, Kirtland Air Force Base, New Mexico. Captain Richard J. Cook (LRO) was the Laboratory Project Officer-in-Charge.

When US Government drawings, specifications, or other data are used for any purpose other than a definitely related Government procurement operation, the Government thereby incurs no responsibility nor any obligation whatsoever, and the fact that the Government may have formulated, furnished, or in any way supplied the said drawings, specifications, or other data, is not to be regarded by implication or otherwise, as in any manner licensing the holder or any other person or corporation, or conveying any rights or permission to manufacture, use, or sell any patented invention that may in any way be related thereto.

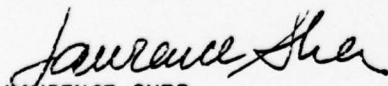
This report has been reviewed by the Information Office (OI) and is releasable to the National Technical Information Service (NTIS). At NTIS, it will be available to the general public, including foreign nations.

This technical report has been reviewed and is approved for publication.

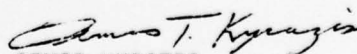


RICHARD J. COOK  
Captain, USAF  
Project Officer

FOR THE COMMANDER



LAWRENCE SHER  
Chief, ALL Beam Control Branch



DEMOS KYRAZIS  
Colonel, USAF  
Chief, Laser Development Division

DO NOT RETURN THIS COPY. RETAIN OR DESTROY.



UNCLASSIFIED

SECURITY CLASSIFICATION OF THIS PAGE (When Data Entered)

| REPORT DOCUMENTATION PAGE   |  | READ INSTRUCTIONS<br>BEFORE COMPLETING FORM |
|---|--|---|
| 1. REPORT NUMBER<br>AFWL-TR-75-84 ✓   | 2. GOVT ACCESSION NO.  | 3. RECIPIENT'S CATALOG NUMBER               |
| 4. TITLE (and Subtitle)<br>ON SPECTROSCOPIC MODELING OF THE WATER MOLECULE.   | 5. TYPE OF REPORT & PERIOD COVERED<br>Final Report, ✓                                  |   |
| 6. AUTHOR(s)<br>D./Rogovin<br>H./Tigelaar   | 7. PERFORMING ORG. REPORT NUMBER   |   |
| 8. PERFORMING ORGANIZATION NAME AND ADDRESS<br>University of Arizona ✓<br>Tucson, Arizona 85721   | 9. CONTRACT OR GRANT NUMBER(s)<br>F29601-74A-0023-0002 new                             |   |
| 10. CONTROLLING OFFICE NAME AND ADDRESS<br>Air Force Weapons Laboratory (LRO)<br>Kirtland Air Force Base, NM 87117  | 11. PROGRAM ELEMENT, PROJECT, TASK AREA & WORK UNIT NUMBERS<br>62601F 1709<br>3326D913 |   |
| 12. MONITORING AGENCY NAME & ADDRESS (if different from Controlling Office)<br>1262p  | 13. REPORT DATE<br>September 1976  |   |
|   | 14. NUMBER OF PAGES<br>60  |   |
|   | 15. SECURITY CLASS. (of this report)<br>UNCLASSIFIED                                   |   |
|   | 16. DECLASSIFICATION/DOWNGRADING SCHEDULE  |   |
| 17. DISTRIBUTION STATEMENT (of this Report)<br>Approved for public release; distribution unlimited.   |  |   |
| 18. DISTRIBUTION STATEMENT (of the abstract entered in Block 20, if different from Report)  |  |   |
| 19. SUPPLEMENTARY NOTES   |  |   |
| 20. KEY WORDS (Continue on reverse side if necessary and identify by block number)<br>Spectroscope<br>Water Molecule<br>Water Vapor   |  |   |
| 21. ABSTRACT (Continue on reverse side if necessary and identify by block number)<br>This report examines the validity of spectroscopic modeling techniques for describing the rotational structure of high lying rotational levels of light asymmetric rotors, such as water. Present techniques based on Watson's rotational Hamiltonian were found to be inadequate. |  |   |

DD FORM 1 JAN 73 1473

EDITION OF 1 NOV 65 IS OBSOLETE

UNCLASSIFIED

SECURITY CLASSIFICATION OF THIS PAGE (When Data Entered)

033800

LB

# CONTENTS

| <u>Section</u> |   | <u>Page</u> |
|----------------|---|-------------|
| I              | INTRODUCTION                              | 1           |
| II             | GENERAL DISCUSSION                        | 3           |
| III            | THE ROTATING MORSE OSCILLATOR             | 6           |
| IV             | NUMERICAL COMPARISON                      | 10          |
| V              | NUMERICAL ANALYSIS FOR THE WATER MOLECULE | 24          |
| VI             | DISCUSSION AND CONCLUSIONS                | 50          |

|                                 |   |
|---------------------------------|---|
| ACCESSION for                   |   |
| NTIS                            | White Section <input checked="" type="checkbox"/> |
| DOC                             | Buff Section <input type="checkbox"/>             |
| UNANNOUNCED                     | <input type="checkbox"/>                          |
| JUSTIFICATION .....             |   |
| BY .....                        |   |
| DISTRIBUTION/AVAILABILITY CODES |   |
| Dist.                           | Avail. and/or SPECIAL                             |
| A                               |   |

# TABLES

| <u>Table</u> |   | <u>Page</u> |
|--------------|---|-------------|
| I            | Values for Rotational - Distortion Coefficients                             | 12          |
| II           | Comparison of Perturbation Expansion to Observed Energy Levels              | 13          |
| III          | Comparison of Rotational - Distortion Coefficients vs. $A_j$                | 16          |
| IV           | Predictions of First 30 Rotational Levels                                   | 17          |
| V            | Distortion Levels from Fitting $J = 6$ to $J = 10$ Levels                   | 18          |
| VI           | Resultant Spectrum  | 19          |
| VII          | Results of Fitting the $J = 11$ to $J = 20$ Rotational Levels               | 22          |
| VIII         | Least Squares Fit for Rotational Constants                                  | 23          |
| IX           | Convergence of the Power Series   | 30          |
| X            | Contribution to Total Rotational Energy of Various Terms of the Hamiltonian | 34          |
| XI           | Test for Uniqueness of Least Squares Fitting for High and Low $\tau$        | 40          |
| XII          | Test for Uniqueness of Least Squares Fitting for $J = 1-8, 10, 11, 12$      | 41          |
| XIII         | Predicability of Various Fits   | 42          |

## SECTION I

### INTRODUCTION

Because of its unique rotation-vibration structure and its dominant role in atmospheric absorption of CO<sub>2</sub> laser radiation, the H<sub>2</sub><sup>16</sup>O molecule has recently been a topic of great interest (refs. 1-10). The internal nuclear motion of this molecule is substantially complicated by the following four features: (1) the large molecular asymmetry; (2) the small moments of inertia (and correspondingly large rotational energies); (3) the extreme anharmonic and low frequency structure of the bending mode vibrations\*; and (4) the large amplitude fluctuations of the bond angle. These features cause water to display strong coupling between the molecular rotations and the bending mode vibration and, in addition, to exhibit large centrifugal distortion effects (ref. 1). These effects manifest themselves not only in the rotation-vibration energy level scheme of water but also in the effective geometric structure. For example, examination of recent high-resolution microwave data (refs. 1,2) reveals that the apparent bond angle deviates over a range of 3.4° depending on which pair of (experimentally determined) inertia constants are used in the analysis. (The apparent bond length deviates over a range of 0.014 Å, which is appreciably less than that of the bond angle.)

Present analysis of high-resolution microwave and far-infrared spectral data involves a least squares fitting to a phenomenological rotational expansion Hamiltonian, first developed by Watson (ref. 11). For virtually all molecular systems of interest, such spectroscopic modeling techniques yield a reliable and useful description of the molecule. However, these techniques, which rely on the rapid convergence of a power series, require that the rotation-vibration interaction and centrifugal distortion be in some sense small. For the particular case

---

\* The experimental energy spacings are 1594.5, 1556.94, and 1515.25 cm<sup>-1</sup> (from refs. 3 and 17).



of water, this is not the case. Thus, one is lead to question the validity of spectroscopic modeling techniques as applied to water. In this report, this question is examined in detail.

Before describing the nature of this work, a brief statement is presented on the results. As is well known, the standard Watson rotational Hamiltonian consists of a series expansion in the components of the angular momentum operator to various powers together with a number of rotation and rotation-distortion coefficients that are to be determined from available experimental data. For light asymmetric molecules such as water, the rotational wave functions depend in a sensitive way on these coefficients. Hence, if one requires accurate wave functions (and therefore, a correct physical description of the molecule), it is important that these coefficients be unique and that the power series expansion be highly convergent. These questions have been examined for two systems: (1) a rotating Morse oscillator and (2) the  $\text{H}_2\text{O}$  molecule itself. We find that for the high-lying states (i.e.,  $J \geq 10$ ) the coefficients are not unique (i.e., they vary with the levels used for fitting), the series expansion does not converge, and the higher order coefficients are devoid of any physical significance. Furthermore, the resultant rotational Hamiltonian has little value with regard to its ability to either predict new energy levels (i.e., states that were not used for fitting purposes) or to determine rotational wave functions that accurately describe the physical state of the molecule. As a consequence, this approach appears to be essentially useless for describing the high-lying states of  $\text{H}_2\text{O}$ . These difficulties arise from and reflect the large rotation-vibration interaction in water and are discussed in detail in this report.

In two companion papers, which were guided and strongly influenced by the findings of this work, the rotation-vibration structure of the water molecule is calculated in a way that directly includes the bending mode.

## SECTION II

### GENERAL DISCUSSION

It is well known that a theoretical analysis of a molecular system undergoing both rotational and vibrational motion, even within the Born-Oppenheimer approximation (ref. 12), is usually difficult. This is especially true for molecular systems that exhibit strong nonlinear vibrational features or significant centrifugal distortion effects, i.e., light molecules such as water.

A number of approaches may be applied to the study of the water molecule. The first would be to determine the electronic wave functions and to use these to calculate the vibrational potential. Using this potential, the nuclear wave equation would then be solved to obtain the rotation-vibration energies and wavefunctions. Unfortunately, the large number of first-principle calculations (ref. 13) of the molecular electronic structure of water have not produced wavefunctions of sufficient accuracy to render this approach useful.

The second approach is to choose a nuclear potential that will fit the experimentally observed vibrational ( $J = 0 \rightarrow J = 0$ ) energy differences. This potential is then combined with the Wilson-Howard (ref. 14) expression for the molecular kinetic energy, and the resulting Hamiltonian is used to obtain the rotation-vibration energy levels and wavefunctions within some suitable approximation. This approach suffers from the fact that the chosen potential usually does not approximate the true potential well enough to predict energy levels to the accuracy of those measured by microwave and high-resolution infrared techniques.

Consequently, most workers (refs. 1,2,15) have used a third approach in which the vibration-rotation Hamiltonian is a polynomial expansion in the components of the total angular momentum. This reduced Hamiltonian has the advantage that it does not require any information about the vibrational motion of the molecular system, as only the angular momentum operators appear in it. Instead, it contains a large number of rotation-

distortion coefficients that must be extracted from the observed spectral line data. In general, an asymmetric rotor such as water requires  $(n + 1)$  distortion coefficients to each order  $n$  of angular momentum operator used to characterize the rotational spectrum within a given vibrational band.

Due to the widespread use of this third approach one would naturally like to check its performance within some model system where analytic solutions are available. Then, by comparing the predictions of the expanded rotational Hamiltonian to that of the model, a measure of its reliability can be obtained. In particular, the following five features should be examined in detail.

(1) In developing a power series in the components of the total angular momentum, what physical parameter  $\eta$  is this expansion based on, i.e., is  $\eta = \text{rotational energy/vibrational energy}$ ?

(2) How meaningful is this characterization, i.e., is this approach limited to the low-lying  $J$  states or is it useful for all rotational levels?

(3) Does the power series converge?

(4) Is the power series expansion unique?

(5) To what extent can this approach predict new energy levels?

In this report, these questions are first examined within the context of a rotating diatomic Morse oscillator. Then, any difficulties that arise in this simple (diatomic) system can be expected to appear to a greater degree in asymmetric polyatomic molecules where the rotational structure exhibits a much greater degree of complexity and in addition, possesses a number of vibrational degrees of freedom as well as coriolis forces.

Also note that for highly asymmetric molecules such as water, the rotational portion of the molecular wavefunction depends sensitively on the various coefficients that appear in the Watson Hamiltonian. As a consequence, questions (2) through (4) are of critical importance for any study that requires accurate wavefunctions. To reinforce the results found in the case of a rotating Morse oscillator, some of the same tests



have also been applied to the water molecule. More precisely, standard techniques were used to construct the Watson Hamiltonian for the  $\text{H}_2\text{O}$  molecule and then questions (2) through (5) were examined for this case.

Chapter 3 of this report reviews those aspects of the rotating Morse oscillator that are relevant for this work, discusses the physical parameter that arises as an expansion coefficient, and examines the limitations of perturbation expansion techniques as they appear for this system. In chapter 4, the predictions of the reduced Hamiltonian are compared to the analytic results. It is found that this approach is not useful in discussing the higher rotational levels ( $J > 10$ ) of light molecules ( $A \sim 10 \text{ cm}^{-1}$ ). Chapter 5 is devoted to the numerical analysis of the Watson Hamiltonian for  $\text{H}_2\text{O}$  as well as a discussion of the findings. Finally, chapter 6 contains our conclusions.

### SECTION III

#### THE ROTATING MORSE OSCILLATOR

Before proceeding, comments are presented on the accuracy of the solutions obtained by Pekeris (ref. 16) for a rotating Morse oscillator. Recall that Pekeris neglected all terms of the form

$$AJ(J+1)(y-1)^3, AJ(J+1)(y-1)^4, \dots$$

from the rotation-vibration Hamiltonian. Here  $A$  is the rotational constant,  $J$  the rotational quantum number, and

$$y = \exp[-\alpha(r - r_e)] \quad (1)$$

In equation (1),  $r_e$  is the equilibrium bond length,  $r$  is the nuclear separation, and  $\alpha$  characterizes the range of the Morse potential  $U_M(r)$ , given by

$$U(r) = D\{1 - \exp[-\alpha(r - r_e)]\}^2 \quad (2)$$

Typically,  $\alpha \approx 1 \text{ \AA}^{-1}$  and  $D$ , the strength of the potential, is about  $38,285 \text{ cm}^{-1}$  for  $\text{H}_2$  and  $37,225 \text{ cm}^{-1}$  for  $\text{HCl}$  (ref. 17). To estimate the size of the leading term, replace the quantity

$$(r - r_e) \rightarrow \langle \sigma r^2 \rangle^{1/2} \quad (3)$$

where  $\langle \sigma r^2 \rangle$  is the mean square deviation of the nuclear separation from  $r_e$  due to either centrifugal distortion or nuclear vibration. (As a rough estimate, note that  $r_e(n=1) = 161/160(r_e)(n=0)$  and  $E_{n=1, J=0} - E_{n=0, J=0} = 1500 \text{ cm}^{-1}$ .) Assume that the stretching of the bond from its equilibrium length varies with the excitation energy of the level of interest (relative to the ground state), then for  $J \leq 40$ ,

$$\sqrt{\langle \sigma r^2 \rangle} \lesssim 5 \times 10^{-2} \text{ \AA} \quad (4)$$

and taking  $\alpha = 1 \text{ \AA}^{-1}$  find that

$$AJ(J+1)(y-1)^3 \lesssim 2 \text{ cm}^{-1} \quad (5)$$

for  $A = 10 \text{ cm}^{-1}$ . By way of comparison, note that the rotational energy of a Morse oscillator for  $J = 40$  is about  $13,000 \text{ cm}^{-1}$  for  $D = 33,000 \text{ cm}^{-1}$  and for  $A = 10 \text{ cm}^{-1}$ . Thus, we may safely use the Pekeris solutions.

Next, the energy spectrum of a rotating Morse oscillator is given by (ref. 16)

$$E_{nJ} = D + c_0 - \frac{(D - \frac{1}{2}c_1)^2}{D + c_2} + \frac{2a(D - \frac{1}{2}c_1)\hbar}{\sqrt{2\mu} (D + c_2)^{1/2}} (n + \frac{1}{2}) - \frac{a^2\hbar^2}{2\mu} (n + \frac{1}{2})^2 \quad (6)$$

where  $n$  is the vibrational quantum number and

$$c_0 = AJ(J+1) \left\{ 1 - \frac{3}{\alpha r_e} + \frac{3}{(\alpha r_e)^2} \right\} \quad (7a)$$

$$c_1 = AJ(J+1) \left\{ \frac{4}{\alpha r_e} - \frac{6}{(\alpha r_e)^2} \right\} \quad (7b)$$

and

$$c_2 = AJ(J+1) \left[ -\frac{1}{\alpha r_e} + \frac{3}{(\alpha r_e)^2} \right] \quad (7c)$$

If one expands equation (6) in powers of  $J(J+1)$ , the first two rotational terms are

$$\frac{E_J}{h} \approx AJ(J+1) - \frac{4A^3}{\omega_0^2} J^2(J+1)^2 \quad (8)$$

where  $\omega_0 = \alpha(D/2\mu)^{1/2}$  is the harmonic frequency, and  $\mu$  is the reduced mass. For the expansion to be physically reasonable one would conclude on the basis of equation (8) that

$$J \ll \left[ \frac{\omega_0}{2A} \right] \quad (9)$$

For light molecules  $\omega_0 \approx 10^3 \text{ cm}^{-1}$  and  $A \approx 10 \text{ cm}^{-1}$  so that  $J \ll 50$ , and one would conclude that the expansion techniques could be useful for  $J \lesssim 15$ . This, however, is somewhat optimistic. An examination of equation (6) reveals that the true expansion parameter  $\eta$  is

$$\eta = \frac{c_2}{D}. \quad (10)$$

For  $\alpha r_e = 1$ , find that a perturbation expansion is valid provided that

$$J \ll \left[ \frac{D}{2A} \right]^{1/2} \quad (11)$$



For  $D = 33 \times 10^3 \text{ cm}^{-1}$  and  $A = 10 \text{ cm}^{-1}$ , this requires that  $J \ll 40$ . Consequently, perturbation expansion techniques are limited to  $J \lesssim 10$ . For states beyond  $J = 10$ , the centripetal distortion energy has become so large that a perturbation expansion based on the rigid rotor approximation requires many terms to converge. As a specific example, consider the level  $J = 20$  for which  $\eta = 0.255$ . To ensure an accuracy of one part in  $10^6$ , it is necessary to include terms of order  $\eta^{12}$  in the perturbation expansion. Now, for a diatomic molecule, the rotational structure is characterized by only one angular momentum operator,  $P^2$ , and such an analysis is possible. On the other hand, the situation is virtually hopeless for asymmetric polyatomic molecules. There, one is faced with a variety of angular momentum operators such as  $P^2$ ,  $P_+^2$ , and  $P_-^2$  plus many combinations such as  $P_+^4 P_-^2$  and so on. In fact, if one goes out to order  $P^{2n}$ , there are  $(2n + 2)$  distortion coefficients. As a specific example, consider water. Note that water has three different moments of inertia of which the two largest are strongly coupled to the bending mode, which can be reasonably well approximated as a Morse oscillator (ref. 5). Then, for the  $J = 16$  level,  $\eta \approx \frac{1}{2}$ , and this requires terms to order  $\eta^{20}$  in order to characterize all of the energy levels from the ground state to  $J = 16$ , to one part in  $10^6$ . This, in turn, implies that one requires a perturbation Hamiltonian, which includes terms of order  $P^{40}$ ; therefore, there are several hundred unknown rotation-distortion constants.

#### SECTION IV

##### NUMERICAL COMPARISON

This section examines the reliability of the power series expansion approach (as generated by the Watson Hamiltonian for a diatomic molecule) in predicting new energy levels and, in addition, tests its uniqueness. The philosophy here is to regard the energy level structure, as generated by equation (6), as an observed spectrum. Then, the rotation-distortion coefficients that appear in the Watson Hamiltonian are fit to the observed low-lying levels. The fit should be to the low-lying levels to ensure that the moment of inertia and the first distortion coefficient have reasonable values. As shall be seen, if one fits to the higher levels, unphysical values are obtained for the distortion coefficients and rotation constants.

For a diatomic molecule, the Watson Hamiltonian reduces to

$$\mathcal{H}_R = A_1 P^2 + A_2 P^4 + A_3 P^6 + \dots \quad (12)$$

where  $P^2$  is the square of the total angular momentum and the  $A_i$  are the rotation distortion coefficients that will depend on the vibrational band but should not vary significantly with the rotational quantum number. Thus, within a given vibrational band, the rotational energy levels are

$$E_J = E_0 + A_1 J(J+1) + A_2 J^2(J+1)^2 + \dots \quad (13)$$

where  $E_0$  is the vibrational energy.

For a specific numerical test, the following values have been chosen for  $D$ ,  $\alpha$ ,  $r_e$ , and  $\mu$ :

$$D = 3.3 \times 10^4 \text{ cm}^{-1}; \quad \alpha = 1.019 \text{ \AA}^{-1}$$

$$r_e = 1.3264 \text{ \AA};$$

$$\mu = 1 \text{ amu.}$$

These values generate a spectrum that roughly describes the low-lying vibrational states of the bending mode of H<sub>2</sub>O (ref. 5).

Recently, De Lucia, Helminger, Cook and Gordy (ref. 1) fit 15 microwave lines of H<sub>2</sub>O in the ground vibrational state using a perturbation expansion that included terms to order  $P^{10}$ . These transitions involved rotational levels as low as  $J = 1$  to as high as  $J = 10$ . The equivalent procedure for the rotating Morse oscillator would be to fit those levels from  $J = 1$  to  $J = 10$  by a perturbation expansion to terms of  $P^{10}$ . Due to the extreme simplicity of the rotational structure of diatomics, this means that the following spectrum

$$E_J = A_1 J(J+1) + A_2 J^2(J+1)^2 + \dots + A_5 J^5(J+1)^5 \quad (14)$$

should be fit to the first 10 levels generated by equation (14). (In equation (14), all energies are measured from the ground rotational state.) Using a least squares fit, the values in table 1 were obtained for the rotational-distortion coefficients. Finally, note that the various coefficients were totally uncorrelated; consequently, they should be highly reliable. (The standard deviations for the rotation coefficients  $B_j$  and  $C_j$  ( $j = 1-5$ ) are zero as one is effectively solving for five unknowns in five linear equations. The standard deviations for the  $A_j$  and  $D_j$  will be nonzero. However, they are extremely small because of the simple character of the energy levels and the fact that we are fitting to only 10 levels.)

A comparison of the perturbation expansion (as embodied in equation (14)) to the observed energy levels is exhibited in table 2 for the first 30 rotational levels. An examination of this table shows that there is a significant deviation by  $J = 13$ , which is only three states and  $656.20 \text{ cm}^{-1}$  above the last level used for fitting purposes. By  $J = 20$ , the energy level structure predicted by the Watson Hamiltonian deviated by more than  $325 \text{ cm}^{-1}$  from the "observed" value. This is an 8% error and is a signal that perturbation expansion techniques are



breaking down. Another indication that this is happening can be seen by comparing the first term in equation (14), i.e., the rigid rotor energy, to the second-order term, the centripetal distortion energy. Thus,

$$A_1 J(J+1) \approx 4000 \text{ cm}^{-1}$$

$$A_2 J^2(J+1)^2 \approx 500 \text{ cm}^{-1}$$

for  $J = 20$ . When this occurs, one must abandon the conceptual picture of a rigid rotor slightly distorted by centripetal forces. Further evidence that the rigid rotor picture is totally inadequate (and therefore the perturbation technique is inadequate) is dramatically displayed by the rotational levels  $J = 22$  and  $J = 23$ , where the predicted energy levels decrease with increasing  $J$ . Finally, by  $J = 27$ , the Watson Hamiltonian predicts negative energy values. The reason for this difficulty can be traced to the fact that for  $J = 27$ , the perturbation expansion parameter  $\eta \approx 0.45$  and many more terms are required if the series is to converge. Also note that the ratio of the fifth term to the first is

$$\left| \frac{A_5 J^5 (J+1)^5}{A_1 J(J+1)} \right| \approx 2$$

which is a clear-cut sign that power series expansion procedures are essentially useless.

Table 1

VALUES FOR ROTATIONAL - DISTORTION COEFFICIENTS

---

|       |  |
|-------|--|
| $A_1$ | $= 9.50271 \times 10^0 \text{ cm}^{-1}$      |
| $A_2$ | $= -1.45207 \times 10^{-3} \text{ cm}^{-1}$  |
| $A_3$ | $= -3.36340 \times 10^{-7} \text{ cm}^{-1}$  |
| $A_4$ | $= +9.11721 \times 10^{-9} \text{ cm}^{-1}$  |
| $A_5$ | $= -4.31392 \times 10^{-11} \text{ cm}^{-1}$ |

---

Table 2

## COMPARISON OF PERTURBATION EXPANSION TO OBSERVED ENERGY LEVELS

| State   | Observed<br>(cm <sup>-1</sup> )* | Expansion<br>(cm <sup>-1</sup> ) <sup>†</sup> | Diff.<br>(cm <sup>-1</sup> ) |
|---------|----------------------------------|---|------------------------------|
| $J = 1$ | 19.036                           | 19.036  | 0.0                          |
| 2       | 57.073                           | 57.072  | -0.001                       |
| 3       | 114.04                           | 114.039                                       | +0.001                       |
| 4       | 189.83                           | 189.832                                       | 0.0                          |
| 5       | 284.31                           | 284.312                                       | 0.0                          |
| 6       | 397.31                           | 397.306                                       | -0.005                       |
| 7       | 528.61                           | 528.613                                       | 0.0                          |
| 8       | 678.00                           | 678.00  | 0.0                          |
| 9       | 845.20                           | 845.20  | 0.0                          |
| 10      | 1029.90                          | 1029.90                                       | 0.0                          |
| 11      | 1231.90                          | 1231.7  | -0.2                         |
| 12      | 1450.7                           | 1450.03                                       | -0.67                        |
| 13      | 1686.1                           | 1684.03                                       | -2.97                        |
| 14      | 1937.6                           | 1932.31                                       | -5.29                        |
| 15      | 2205.0                           | 2192.58                                       | -12.42                       |
| 16      | 2487.6                           | 2661.11                                       | -17.49                       |
| 17      | 2785.3                           | 2731.93                                       | -53.37                       |
| 18      | 3097.5                           | 2995.68                                       | -101.82                      |
| 19      | 3423.8                           | 3238.03                                       | -185.77                      |
| 20      | 3763.8                           | 3437.54                                       | -326.26                      |
| 21      | 4117.1                           | 3562.84                                       |                              |
| 22      | 4483.2                           | 3568.85                                       |                              |
| 23      | 4861.7                           | 3392.00                                       |                              |
| 24      | 5252.2                           | 2944.12                                       |                              |
| 25      | 5654.2                           | 2104.67                                       |                              |
| 26      | 6067.4                           | 711.87  |                              |
| 27      | 6491.4                           | -1452.64                                      |                              |
| 28      | 6925.7                           | -4671.43                                      |                              |
| 29      | 7370.0                           | -9315.79                                      |                              |
| 30      | 7823.9                           | -15863.5                                      |                              |

\*0.01 cm<sup>-1</sup>  $\approx$  50 MHz fitted from analytic solution†For  $p = 0$  band only expansion to  $F^{10}$

The rotation-distortion coefficients as derived from different levels are not unique. Table 3 shows a comparison of these rotational-distortion coefficients used to fit the first five levels (denoted by  $B_j$ ) versus the  $A_j$ . Since the  $B_j$  were fitted to the first five rotational levels, they are nearly equivalent to the Taylor series expansion of equation (6) to  $P^{10}$  [i.e., to  $J^5(J+1)^5$ ] and, consequently, they are the exact values to order  $\eta^6$ , i.e., approximately one part in  $10^{11}$ . Now,  $B_1 = \hbar^2/2\mu r_e^2$  is the rotation constant, and the corresponding  $A$ -coefficient deviates from the correct value by three parts in  $10^4$ . This is far more serious than it appears because these coefficients are often quoted to parts in  $10^6$ . Furthermore, this deviation would lead to an incorrect value of the molecular size by parts in  $10^4$ . Next, consider the first distortion coefficient where a deviation of over 2% is found. Again, this is serious because these coefficients are quoted to parts in  $10^4$ . A further examination of table 3 reveals that there is almost no relationship between the two sets of coefficients beyond  $j = 2$ . Thus,  $B_5$  is almost 30 times the size of  $A_5$ , and they are of opposite signs. One might argue that for low-lying levels this is not too important. Consider, however,  $J = 10$ . Then,

$$A_5 J^5 (J+1)^5 \approx -0.430 \text{ cm}^{-1}$$

$$B_5 J^5 (J+1)^5 \approx +12.3 \text{ cm}^{-1}$$

and for  $J = 20$

$$A_5 J^5 (J+1)^5 = -430 \text{ cm}^{-1}$$

$$B_5 J^5 (J+1)^5 = +12,300 \text{ cm}^{-1}$$

Note, that the energy associated with the  $P^{10}$  term is about three times that associated with the rigid rotor energy. The implications of this

in regard to calculating asymmetric rotor wavefunctions for  $\text{H}_2\text{O}$  are significant because these wavefunctions depend sensitively on the rotation-distortion constant. Also note that the large discrepancy between these two terms implies that the expansion techniques are valid only for low-lying states where the lower order terms dominate the level structure. Finally, in table 4 are listed the predictions of the first 30 rotational levels using  $B_1, \dots, B_5$ .

The distortion coefficients are *very* sensitive to the levels that are used for fitting purposes. Table 5 shows the distortion coefficients that arise when one fits the  $J = 6$  to  $J = 10$  levels. These coefficients are denoted by  $C_J$ . Notice that significant deviations appear immediately. For example, the rotation constant is off by almost one part in  $10^4$ , and is larger, not smaller, than  $B_0$ . This is quite serious because the first coefficient is directly related to the moment of inertia. Now, as the molecule rotates faster and faster, it gradually opens up, i.e., it stretches, which increases its moment of inertia. Consequently, if one fits the rotation-distortion coefficients to highly excited rotational states, a larger moment of inertia would be expected and, therefore, a smaller rotation constant. Instead, we find that

$$C_0 > B_0.$$

The first distortion coefficient is off by 2%. Also, the last two coefficients are between one and two orders of magnitude too small. Thus, one may draw the conclusion that the distortion coefficients are not only not unique, but they vary in a sensitive and nonphysical manner with whichever states are used for fitting purposes. Also note that the large difference in size of the higher order distortion constants casts doubt on their physical meaning. Finally, the resultant spectrum is displayed in table 6.

Table 3

COMPARISON OF ROTATIONAL - DISTORTION COEFFICIENTS VS.  $A_j$ 

| $J$ | $B_j(\text{cm}^{-1})$     | $A_j(\text{cm}^{-1})$      | $B_j - A_j(\text{cm}^{-1})$ | $(B_j - A_j)/A_j$     |
|-----|---------------------------|----------------------------|-----------------------------|-----------------------|
| 1   | 9.52101                   | 9.52071                    | +0.0030                     | $3.14 \times 10^{-4}$ |
| 2   | $-1.48844 \times 10^{-3}$ | $-1.45207 \times 10^{-3}$  | $-0.0313 \times 10^{-3}$    | $2.1 \times 10^{-2}$  |
| 3   | $+1.58233 \times 10^{-6}$ | $-3.36340 \times 10^{-7}$  | $+1.94573 \times 10^{-6}$   | 5.7                   |
| 4   | $-6.94441 \times 10^{-8}$ | $9.11721 \times 10^{-9}$   | $-7.856 \times 10^{-8}$     | 8.6                   |
| 5   | $1.24007 \times 10^{-9}$  | $-4.31392 \times 10^{-11}$ | $+1.2833 \times 10^{-9}$    | 29                    |



Table 4

## PREDICTIONS OF FIRST 30 ROTATIONAL LEVELS

| $J$ | Expansion ( $\text{cm}^{-1}$ ) | Observed ( $\text{cm}^{-1}$ ) |
|-----|--------------------------------|-------------------------------|
| 1   | $1.90361 \times 10^1$          | 19.036                        |
| 2   | $5.70729 \times 10^1$          | 57.073                        |
| 3   | $1.14040 \times 10^2$          | 114.04                        |
| 4   | $1.89832 \times 10^2$          | 189.83                        |
| 5   | $2.84211 \times 10^2$          | 284.31                        |
| 6   | $3.97327 \times 10^2$          | 397.31                        |
| 7   | $5.28799 \times 10^2$          | 528.61                        |
| 8   | $6.78941 \times 10^2$          | 678.00                        |
| 9   | $8.48787 \times 10^2$          | 845.20                        |
| 10  | $1.04126 \times 10^3$          | 1029.90                       |
| 11  | $1.26316 \times 10^3$          | 1231.90                       |
| 12  | $1.52860 \times 10^3$          | 1450.7                        |
| 13  | $1.86463 \times 10^3$          | 1686.1                        |
| 14  | $2.32000 \times 10^3$          | 1937.6                        |
| 15  | $2.97844 \times 10^3$          | 2205.0                        |
| 16  | $3.97787 \times 10^3$          | 2487.6                        |
| 17  | $5.53791 \times 10^3$          | 2785.3                        |
| 18  | $7.99781 \times 10^3$          | 3097.5                        |
| 19  | $1.18682 \times 10^4$          | 3423.8                        |
| 20  | $1.78999 \times 10^4$          | 3763.8                        |
| 21  | $2.71751 \times 10^4$          | 4117.1                        |
| 22  | $4.12240 \times 10^4$          | 4483.2                        |
| 23  | $6.21757 \times 10^4$          | 4861.7                        |
| 24  | $9.29479 \times 10^4$          | 5252.2                        |
| 25  | $1.37484 \times 10^5$          | 5654.2                        |
| 26  | $2.01048 \times 10^5$          | 6067.4                        |
| 27  | $2.90584 \times 10^5$          | 6491.4                        |
| 28  | $4.15160 \times 10^5$          | 6925.7                        |
| 29  | $5.86494 \times 10^5$          | 7370.0                        |
| 30  | $8.19598 \times 10^5$          | 7823.9                        |

$B$  constants are :  $9.52101$ ,  $-1.48444 \times 10^{-3}$ ,  $1.58233 \times 10^{-6}$ ,  
 $-6.94441 \times 10^{-6}$ , and  $1.24007 \times 10^{-9}$

Table 5

DISTORTION LEVELS FROM FITTING  $J = 6$  TO  $J = 10$  LEVELS

| $J$<br>— | $B_J(\text{cm}^{-1})$<br>— | $C_J(\text{cm}^{-1})$<br>— |
|----------|----------------------------|----------------------------|
| 1        | 9.52101                    | 9.52187                    |
| 2        | $-1.4844 \times 10^{-3}$   | $-1.52611 \times 10^{-3}$  |
| 3        | $1.5823 \times 10^{-6}$    | $+1.40507 \times 10^{-6}$  |
| 4        | $-6.9444 \times 10^{-8}$   | $-9.0708 \times 10^{-9}$   |
| 5        | $1.2401 \times 10^{-9}$    | $2.83792 \times 10^{-11}$  |



Table 6  
RESULTANT SPECTRUM

| $J$ | Expansion( $\text{cm}^{-1}$ ) | Observed ( $\text{cm}^{-1}$ ) |
|-----|-------------------------------|-------------------------------|
| 1   | $1.90375 \times 10^1$         | 19.036                        |
| 2   | $5.70768 \times 10^1$         | 57.073                        |
| 3   | $1.14047 \times 10^2$         | 114.04                        |
| 4   | $1.89843 \times 10^2$         | 189.83                        |
| 5   | $2.84324 \times 10^2$         | 284.31                        |
| 6   | $3.97320 \times 10^2$         | 397.31                        |
| 7   | $5.28626 \times 10^2$         | 528.61                        |
| 8   | $6.78011 \times 10^2$         | 678.00                        |
| 9   | $8.45213 \times 10^2$         | 845.20                        |
| 10  | $1.02995 \times 10^3$         | 1029.90                       |
| 11  | $1.23190 \times 10^3$         | 1231.90                       |
| 12  | $1.45074 \times 10^3$         | 1450.7                        |
| 13  | $1.68611 \times 10^3$         | 1686.1                        |
| 14  | $1.93765 \times 10^3$         | 1937.6                        |
| 15  | $2.20496 \times 10^3$         | 2205.0                        |
| 16  | $2.48764 \times 10^3$         | 2487.6                        |
| 17  | $2.78529 \times 10^3$         | 2785.3                        |
| 18  | $3.09748 \times 10^3$         | 3097.5                        |
| 19  | $2.42379 \times 10^3$         | 3423.8                        |
| 20  | $3.76380 \times 10^3$         | 3763.8                        |
| 21  | $4.11709 \times 10^3$         | 4117.1                        |
| 22  | $4.48328 \times 10^3$         | 4483.2                        |
| 23  | $4.86198 \times 10^3$         | 4861.7                        |
| 24  | $5.25286 \times 10^3$         | 5252.2                        |
| 25  | $5.65566 \times 10^3$         | 5654.2                        |
| 26  | $6.07018 \times 10^3$         | 6067.4                        |
| 27  | $6.49635 \times 10^3$         | 6491.4                        |
| 28  | $6.93423 \times 10^3$         | 6925.7                        |
| 29  | $7.38407 \times 10^3$         | 7370.0                        |
| 30  | $2.84638 \times 10^3$         | 7823.9                        |
| 31  | $8.32198 \times 10^3$         | 8287.1                        |
| 32  | $8.81208 \times 10^3$         | 8759.2                        |
| 33  | $9.31837 \times 10^3$         | 9239.9                        |
| 34  | $9.84318 \times 10^3$         | 9728.9                        |
| 35  | $1.03896 \times 10^4$         | 10226                         |
| 36  | $1.09615 \times 10^4$         | 10730                         |
| 37  | $1.15641 \times 10^4$         | 11242                         |
| 38  | $1.22038 \times 10^4$         | 11762                         |
| 39  | $1.28886 \times 10^4$         | 12288                         |
| 40  | $1.36284 \times 10^4$         | $1.2821 \times 10^4$          |

To show how misleading perturbation expansion techniques can be, table 7 shows the results of fitting the  $J = 11$  to  $J = 20$  rotational levels in the ground vibrational state. The rotational constants, denoted by  $D_J$ , were found by a least squares fit displayed in table 8.

At first glance it would appear that this fit is far better than the previous one in which the spectrum was fit to the first 10 rotational levels. This, however, is not the case. An examination of table 7 reveals that

$$D_0 > B_0,$$

which is opposite to what would be expected. Another disturbing feature of table 8 is that the last three coefficients are more than an order of magnitude smaller than the  $B$  values, and the last coefficient is three orders of magnitude smaller. These features reinforce the conclusion that the higher-order rotation distortion coefficients, generated by the Watson Hamiltonian, are devoid of all physical significance for light molecular systems that are excited to high rotational states. They are, in fact, just a sequence of numbers that are chosen to give a fit of a power series expansion of the form

$$E = \sum_n C_n J^n (J+1)^n$$

to the rotational levels. It does this by vastly decreasing the magnitude of the higher-order rotation-distortion coefficients, as these coefficients have the greatest weight associated with them for high  $J$ . Furthermore, note that if one examines even higher lying rotational states, deviations again arise, e.g., by  $J = 40$ , the discrepancy is over  $800 \text{ cm}^{-1}$ . Also, note that the low-lying levels are in reasonable agreement. This arises because the energy of these states is determined by the first few rotation-distortion coefficients, which are always

correct within parts in  $10^4$ . Finally, note that the  $J = 8, 9, 10$  states are in agreement because they lie near the levels used for the purpose of fitting.

In summary, within the context of the rotating Morse oscillator, the perturbation expansion technique, when applied to highly excited rotational states of light molecules, is devoid of any physical significance. This arises from the fact that the perturbation expansion parameter  $\eta = 2AJ(J + 1)/D$  becomes large ( $\sim \frac{1}{4}$  to  $\frac{1}{2}$ ) for light molecules near  $J = 10$ . As a consequence, the series is a slowly convergent one requiring many terms. Attempts to fit the energy spectrum with just a few terms can be done only by significantly changing the distortion coefficients so that they bear little resemblance to reality. This is borne out by the fact that if one examines even higher levels, the predicted spectrum is still incorrect by hundreds of wave numbers. Thus, the perturbation expansion technique cannot predict new energy levels. Furthermore, it is clear that one can characterize only the low-lying levels (where the rotational distortion energy is small compared to the total rotational energy) by means of the Watson Hamiltonian approach. Also note that the results are not unique, i.e., if one fits the  $J = 1$  to  $J = 5$  levels or the  $J = 6$  to  $10$ , different distortion coefficients are found.

Table 7

RESULTS OF FITTING THE  $J = 11$  TO  $J = 20$  ROTATIONAL LEVELS

| $J$ | Expansion ( $\text{cm}^{-1}$ ) | Observed ( $\text{cm}^{-1}$ ) |
|-----|--------------------------------|-------------------------------|
| 1   | $1.90376 \times 10^1$          | 19.036                        |
| 2   | $5.70766 \times 10^1$          | 57.073                        |
| 3   | $1.14045 \times 10^2$          | 114.04                        |
| 4   | $1.89837 \times 10^2$          | 189.83                        |
| 5   | $2.84314 \times 10^2$          | 284.31                        |
| 6   | $3.97306 \times 10^2$          | 397.31                        |
| 7   | $5.28612 \times 10^2$          | 528.61                        |
| 8   | $6.77999 \times 10^2$          | 678.00                        |
| 9   | $8.45204 \times 10^2$          | 845.20                        |
| 10  | $1.02994 \times 10^3$          | 1029.90                       |
| 11  | $1.23191 \times 10^3$          | 1231.90                       |
| 12  | $1.45086 \times 10^3$          | 1450.7                        |
| 13  | $1.68662 \times 10^3$          | 1686.1                        |
| 14  | $1.93927 \times 10^3$          | 1937.6                        |
| 15  | $2.20929 \times 10^3$          | 2205.0                        |
| 16  | $2.49795 \times 10^3$          | 2487.6                        |
| 17  | $2.80771 \times 10^3$          | 2785.3                        |
| 18  | $3.14295 \times 10^3$          | 3097.5                        |
| 19  | $3.51088 \times 10^3$          | 3423.8                        |
| 20  | $3.92288 \times 10^3$          | 2763.8                        |
| 21  | $4.39623 \times 10^3$          | 4117.1                        |
| 22  | $4.95641 \times 10^3$          | 4483.2                        |
| 23  | $5.64011 \times 10^3$          | 4861.7                        |
| 24  | $6.49903 \times 10^3$          | 5252.2                        |
| 25  | $7.60476 \times 10^3$          | 5654.2                        |
| 26  | $9.05482 \times 10^3$          | 6067.4                        |
| 27  | $1.09801 \times 10^4$          | 6491.4                        |
| 28  | $1.35543 \times 10^4$          | 6925.7                        |
| 29  | $1.70049 \times 10^4$          | 7370.0                        |
| 30  | $2.16265 \times 10^4$          | 7823.9                        |
| 31  | $2.77978 \times 10^4$          | 8287.1                        |
| 32  | $3.60001 \times 10^4$          | 8759.2                        |
| 33  | $4.68405 \times 10^4$          | 9239.9                        |
| 34  | $6.10790 \times 10^4$          | 9728.9                        |
| 35  | $7.96599 \times 10^4$          | 10226                         |
| 36  | $1.03749 \times 10^5$          | 10730                         |
| 37  | $1.34774 \times 10^5$          | 11242                         |
| 38  | $1.74478 \times 10^5$          | 11762                         |
| 39  | $2.24972 \times 10^5$          | 12288                         |
| 40  | $2.88803 \times 10^5$          | $1.2821 \times 10^4$          |



Table 8

## LEAST SQUARES FIT FOR ROTATIONAL CONSTANTS

| $J$ | $B_j(\text{cm}^{-1})$       | $D_j(\text{cm}^{-1})$       | $(B_j - D_j)(\text{cm}^{-1})$ |
|-----|-----------------------------|-----------------------------|-------------------------------|
| 1   | +9.52101                    | 9.52170                     | -0.00069                      |
| 2   | -1.4844 x 10 <sup>-3</sup>  | -1.4871 x 10 <sup>-3</sup>  | +0.003 x 10 <sup>-3</sup>     |
| 3   | +1.5823 x 10 <sup>-6</sup>  | +4.4446 x 10 <sup>-7</sup>  | 1.1378 x 10 <sup>-6</sup>     |
| 4   | -6.94444 x 10 <sup>-8</sup> | -2.5619 x 10 <sup>-9</sup>  | -6.6832 x 10 <sup>-9</sup>    |
| 5   | 1.24007 x 10 <sup>-10</sup> | +1.6066 x 10 <sup>-11</sup> | 1.2384 x 10 <sup>-10</sup>    |

## SECTION V

### NUMERICAL ANALYSIS FOR THE WATER MOLECULE

In the previous two sections the validity of power series expansion techniques was examined for a model system. In this section, similar tests are applied to a real polyatomic asymmetric molecule, namely  $\text{H}_2\text{O}$ . Owing to the mathematical complexity of extreme asymmetric rotors, no analytic work appears possible. Hence, the convergence, uniqueness, and predictability of power series expansion techniques have only been examined numerically.

There are several techniques used in analyzing the Watson rotation Hamiltonian. The simplest consists of a least squares analysis to derive the various rotation-distortion coefficients. The resulting Hamiltonian is then used to derive energy levels within a rigid asymmetric rotor basis (as determined by the  $A$ ,  $B$ , and  $C$  rotation constants), and no attempt is made to diagonalize the rotation Hamiltonian. A second approach, perhaps the most widely used, involves a matrix diagonalization in addition to a least squares analysis. In the appendix, it is shown that a matrix diagonalization does not give rise to significant changes from a linearized analysis. Finally, a third technique, used by De Lucia, et al., is designed to extract out higher order distortion energies from the distortion coefficients. This approach is discussed in reference 1 and we have found it to be far superior to the first two. Nevertheless, it has a number of defects insofar as  $\text{H}_2\text{O}$  is concerned. In general, the numerical results for  $\text{H}_2\text{O}$  confirm the findings for the rotating Morse oscillator; namely, one cannot deduce an adequate physical picture of the molecule without explicitly including the coupling of the vibrational motion of the nuclei to the molecular rotation.

#### CONVERGENCE OF THE POWER SERIES

As a first check on the usefulness and validity of power series expansions, we have examined the rate at which these series converge.

This is an essential test because if the perturbation expansion (about a rigid asymmetric rotor) is to be meaningful it must converge rapidly. Although any criteria devised for convergence are to some degree arbitrary, each term in the series should, in general, be about one order of magnitude smaller than the term proceeding it. Then, for a rotational level that lies about one thousand wave numbers above the rotational ground state, the sum of the energies of all the tenth-order terms (to date, these are the highest order terms used) should be on the order of one-tenth of a wave number. This, in turn, ensures an accuracy of between one-hundredth and one-tenth of a wave number.

As a specific example, the rotational Hamiltonian given by De Lucia, et al., (refs. 1,2) was used to calculate the energy contribution that arises in each order. The various rotation and rotation-distortion constants that appear were obtained from microwave and infrared data involving the low-lying rotational states. Consequently, it should be the most accurate Hamiltonian available, and any convergence problems that arise here should also appear with other Watson Hamiltonians. One might argue that these constants should be extracted from data that include higher rotational levels. However, the resulting Hamiltonian is less accurate, and this point is more thoroughly discussed in the next subsection.

The convergence calculation was carried out in a rigid asymmetric rotor basis. More precisely, we evaluated the diagonal contribution of each term of the Hamiltonian of De Lucia, et al., using the eigenfunctions of an asymmetric rotor with rotation constants

$$\begin{aligned} A &= 27.8806 \text{ cm}^{-1} \\ B &= 14.5217 \text{ cm}^{-1} \\ C &= 9.27769 \text{ cm}^{-1}. \end{aligned}$$

---

Note: References 1 and 2 are concerned only with the low energy states. The results of reference 12 are used only to illustrate the point that many higher order terms ( $P^{12}$ ,  $P^{14}$ , etc.) must be included in the Watson Hamiltonian to adequately describe the water molecule for the higher order state.



This corresponds to a linear analysis instead of a matrix diagonalization. However, the difference between the energies obtained using a linear analysis and matrix diagonalized energies is generally less than  $0.05 \text{ cm}^{-1}$  for all states through  $J$  equals 10 and under five wave numbers for all rotational states through  $J$  equals 16.

Table 9 lists all the various contributions to the energy for all rotational levels through  $J$  equals 10. Here,  $E_R$  refers to the rigid rotor energy,  $E_4$ ,  $E_6$ ,  $E_8$ , and  $E_{10}$  to the fourth, sixth, eighth, and tenth order perturbation energies, and  $E_T$  is the total calculated energy. The next to last column refers to the experimental value of the energy as deduced from spectroscopic data (ref. 18), and  $\Delta E$  is equal to the difference between the matrix diagonalized energy and the linearized energy. All energies are in units of wave numbers.

Recall that our analysis in chapter 2 indicates that the perturbation expansion parameter  $\eta$  was

$$\eta = 2AJ(J + 1)/D \quad (5.1)$$

where  $AJ(J + 1)$  is the rigid rotor energy and  $D$  is the strength of the Morse potential. As mentioned in chapter 2, the bending mode of  $\text{H}_2\text{O}$  can be approximated by a Morse oscillator, and it is reasonable to adopt equation (5.1) as the expansion parameter for this case, although the coefficient (i.e., the factor of 2) is undoubtedly different. Consequently, take

$$\eta_{\text{H}_2\text{O}} = C \frac{(000)\text{ground state asymmetric rotor energy}}{33,000 \text{ cm}^{-1}} \quad (5.2)$$

as the expansion parameter. Here,  $C$  is a numerical factor that lies between 1 and 5, say, and we have taken  $D$  equal to  $3.3 \times 10^4 \text{ cm}^{-1}$ . Then, for  $C = 3$  and a rigid rotor energy of  $2750 \text{ cm}^{-1}$ , the fifth-order energy would be approximately a few wave numbers. For  $\text{H}_2\text{O}$ , convergence difficulties would arise at the 10<sub>7</sub> level.

An examination of table 9 reveals that the tenth order perturbation energies of all the rotational levels through  $J = 6$  are one-tenth of a wave number or less. Beyond  $J = 6$ , there are a number of

levels that do not converge as rapidly. For example, consider the  $7_7$  and  $7_6$  states, where the terms decrease by a factor of 5 only, and the last term is  $0.5 \text{ cm}^{-1}$ . This is approximately 2 orders of magnitude greater than  $\Delta E$  and, consequently, cannot be attributed to the fact that only a linearized calculation was carried out. Instead, it implies that at least for this level, twelveth-order terms should be included. Deviations for such low levels might be attributed to the fact that the microwave data used by De Lucia, et al., contained information on only the low  $\tau$  states and, consequently, difficulties might be expected for high  $\tau$  states. Another possibility is that the effective expansion parameter given by equation (5.2) is sufficiently large to prevent convergence. This would be the case for  $C \approx 4$ . The situation for  $J = 8$  is similar, although somewhat worse. Here, the  $8_5$  and  $8_6$  states have tenth-order energies that are approximately half a wave number, and the  $8_7$  and  $8_8$  levels are two wave numbers. In both cases, the convergence is slow, which implies that  $P^{12}$  and, possibly,  $P^{14}$  terms should be included in the rotational Hamiltonian.

Further examination of table 9 reveals that convergence problems arise for the  $9_4$  through the  $9_9$  states. Also, the  $10_5$  through  $10_{10}$  states all have tenth-order energies that are greater than one wave number. An adequate description of these levels would probably require  $P^{12}$  and  $P^{14}$  order terms and in some cases, possibly,  $P^{16}$  due to the slow convergence.

One might argue that since these levels differ by only a few tenths of a wave number from the observed energies, a tenth-order Hamiltonian is actually sufficient. However, this argument is misleading. The higher-order energies of those states that are well described by this Hamiltonian (i.e., all levels through  $J = 6$  and all the small  $\tau$  levels) have tenth-order energies that are vanishingly small. Also note that these are the levels that are involved in the microwave data, which contain no information on the high  $J_\tau$  states. The total energies of the states agree reasonably well with experiment because these levels lie only a few hundred wave numbers away from the measured ones.

Table 10 lists levels that lie between  $J = 11$  and  $J = 16$  in which the fifth-order term is greater than  $1 \text{ cm}^{-1}$ . In a few isolated cases, this difficulty might be attributed to the fact that

a linear analysis was performed instead of an exact matrix diagonalization. However, in the vast majority of cases, this is not true as is borne out by the analysis in the appendix. In general, the matrix diagonalization gives rise to a correction of under  $1 \text{ cm}^{-1}$ .

Consider, first, the  $J = 11$  levels. For the high  $\tau$  states, i.e.,  $\tau = 7$  to 11, the convergence factor for the last few terms is about 3. Since  $E_{10} \approx 45 \text{ cm}^{-1}$  for  $\tau = 11, 10$  and  $E_{10} \approx 18 \text{ cm}^{-1}$  for  $\tau = 8, 9$ , one would have to include terms of order  $P^{18}$  to describe all the  $J = 11$  levels and retain spectroscopic accuracy for the microwave spectrum. Another interesting feature displayed in table 10 is that although the total energy of the various states is often incorrect by only a few tenths of a wave number from the observed energy, the series do not converge. Presumably, the higher order terms alternate in sign so that their effect on  $E_T$  is small or higher order effects are being included in the lower coefficients. For example, the  $\tau = 6$  and 7 levels could require an  $E_{12}$  as well as an  $E_{14}$  although  $|E_T - E_{\text{OBS}}| = 0.26 \text{ cm}^{-1}$ . (Although the convergence is poor for the high  $\tau$  states of the  $J = 11$  levels, the physical picture of a rigid rotor slightly perturbed by distortion is still viable.)

For  $J = 12$  to 14 the situation is similar except that the convergence is now about 2 for the high  $\tau$  states, and the  $E_{10}$  terms have grown in both absolute magnitude as well as relative size in comparison to  $E_R$ . For these states, the physical picture of an asymmetric rotor slightly perturbed by the rotation-vibration interaction is no longer valid. This is reflected by the fact that for  $J_\tau = 13_{13}$ ,  $E_{10}$  is 5% of the rigid rotation energy. Owing to the slow rate of convergence of the rigid-rotor model, it is virtually impossible to describe these states accurately and still retain a detailed picture of the microwave spectrum.

For the high-lying  $\tau$  levels of the states with  $J = 15$ , there is no convergence. In some situations, higher order rotation-distortion terms are larger in magnitude than some of the lower order ones. Another feature is that states with  $\tau < 0$  are not converging rapidly. Such states do not have a great deal of rotation-vibration interaction and probably could be correctly described if  $P^{12}$  and  $P^{14}$  terms were

included. Furthermore, for  $J = 16$  the situation is essentially the same. However, a new feature has appeared. States that lie lower in energy than the  $J = 15$  states no longer satisfy the criteria. Thus, the  $\tau = -10$  state lies lower in energy than the  $15_{-3}$  level, and it does not meet our convergence requirements. Finally, on the basis of the trend in table 10, it appears likely that for  $J \geq 17$ , convergence difficulties will arise for all  $\tau$ -states.

#### UNIQUENESS

Next, we examine the dependence (if any) of the rotation and higher order distortion constants on the particular set of energy levels used to obtain them. In this test, no attempt was made to remove the effects of the rotation-vibration interaction from these coefficients (as was done in reference 12). Instead, a least squares analysis was carried out on the rotation and higher order distortion constants of the Hamiltonian

$$\begin{aligned}
 \mathcal{H} = & \frac{1}{2}(B + C) P^2 + [A - \frac{1}{2}(B + C)] (P_z^2 - b^2 P_-^2) \\
 & - \Delta_J P^4 - \Delta_{JK} P_z^2 P_-^2 - \Delta_K P^4 - 2\delta_J P_z^2 P_-^2 - \delta_K (P_z^2 P_-^2 + P_-^2 P_z^2) \\
 & + H_J P^6 + H_{JK} P_z^4 P_-^2 + H_{KJ} P_z^2 P_-^4 + H_K P_z^6 + 2h_J P_z^4 P_-^2 \\
 & + h_{JK} P_z^2 (P_z^2 P_-^2 + P_-^2 P_z^2) + h_K (P_z^4 P_-^2 + P_-^2 P_z^4) \\
 & + L_{JK} P_z^4 P_-^4 + L_{KKJ} P_z^2 P_-^6 + L_K P_z^8 + l_K (P_z^6 P_-^2 + P_-^2 P_z^6) \\
 & + P_{Kz} P^{10} + P_K (P_z^8 P_-^2 + P_-^2 P_z^8),
 \end{aligned} \tag{5.3}$$

to ensure that the energy levels of a selected set of states of equation (5.3) agree with available experimental data. This approach has been used by a number of workers, and results of this work reveal some of the limitations inherent in it.



Table 9

## CONVERGENCE OF THE POWER SERIES

| $J$ | $\tau$ | $E_R$   | $E_4$                     | $E_6$                     | $E_8$                     | $E_{10}$                   | $E_T$   | Observed | $\Delta E$ |
|-----|--------|---------|---------------------------|---------------------------|---------------------------|----------------------------|---------|----------|------------|
| 1   | -1     | 23.799  | -5.016 x 10 <sup>-3</sup> | 4.178 x 10 <sup>-6</sup>  | 0                         | 0                          | 23.794  | 23.791   | 0.0        |
| 1   | 0      | 37.158  | -2.118 x 10 <sup>-2</sup> | 1.715 x 10 <sup>-5</sup>  | 3.988 x 10 <sup>-5</sup>  | -8.005 x 10 <sup>-10</sup> | 37.137  | 37.137   | 0.0        |
| 1   | +1     | 42.402  | -3.071 x 10 <sup>-2</sup> | 1.609 x 10 <sup>-4</sup>  | -1.401 x 10 <sup>-6</sup> | 4.270 x 10 <sup>-9</sup>   | 42.372  | 42.361   | 0.0        |
| 2   | -2     | 70.133  | -4.145 x 10 <sup>-2</sup> | -3.234 x 10 <sup>-4</sup> | 2.488 x 10 <sup>-5</sup>  | -2.734 x 10 <sup>-7</sup>  | 70.091  | 70.088   | 0.0        |
| 2   | -1     | 79.513  | -1.652 x 10 <sup>-2</sup> | -1.608 x 10 <sup>-4</sup> | 3.078 x 10 <sup>-7</sup>  | -5.871 x 10 <sup>-9</sup>  | 79.496  | 79.496   | 0.0        |
| 2   | 0      | 95.245  | -6.948 x 10 <sup>-2</sup> | 3.302 x 10 <sup>-4</sup>  | -5.096 x 10 <sup>-6</sup> | 9.340 x 10 <sup>-9</sup>   | 95.176  | 95.174   | 0.0        |
| 2   | +1     | 135.322 | -4.26 x 10 <sup>-1</sup>  | 6.246 x 10 <sup>-3</sup>  | -1.267 x 10 <sup>-4</sup> | 1.776 x 10 <sup>-6</sup>   | 134.902 | 134.902  | 0.0        |
| 2   | +2     | 136.587 | -4.299 x 10 <sup>-1</sup> | 6.682 x 10 <sup>-3</sup>  | -1.516 x 10 <sup>-4</sup> | 2.050 x 10 <sup>-6</sup>   | 136.164 | 136.161  | 0.0        |
| 3   | -3     | 136.889 | -1.262 x 10 <sup>-1</sup> | -1.370 x 10 <sup>-3</sup> | 1.064 x 10 <sup>-4</sup>  | -1.209 x 10 <sup>-6</sup>  | 136.762 | 136.765  | 0.0        |
| 3   | -2     | 142.331 | -5.082 x 10 <sup>-2</sup> | 1.398 x 10 <sup>-3</sup>  | 1.561 x 10 <sup>-4</sup>  | -4.020 x 10 <sup>-6</sup>  | 142.279 | 142.274  | 0.0        |
| 3   | -1     | 173.597 | -2.311 x 10 <sup>-1</sup> | -8.919 x 10 <sup>-5</sup> | 1.838 x 10 <sup>-4</sup>  | -4.903 x 10 <sup>-6</sup>  | 173.367 | 173.370  | -0.001     |
| 3   | 0      | 206.720 | -4.232 x 10 <sup>-1</sup> | 4.796 x 10 <sup>-3</sup>  | -1.712 x 10 <sup>-4</sup> | 1.776 x 10 <sup>-6</sup>   | 206.302 | 206.303  | 0.0        |
| 3   | +1     | 212.627 | -4.776 x 10 <sup>-1</sup> | 7.068 x 10 <sup>-1</sup>  | -2.775 x 10 <sup>-4</sup> | 2.986 x 10 <sup>-6</sup>   | 212.157 | 212.162  | 0.0        |
| 3   | +2     | 287.339 | -2.191 x 10 <sup>0</sup>  | -7.457 x 10 <sup>-2</sup> | -5.469 x 10 <sup>-3</sup> | 1.064 x 10 <sup>-4</sup>   | 285.219 | 285.217  | +0.001     |
| 3   | +3     | 287.537 | -2.186                    | 7.480 x 10 <sup>-2</sup>  | -3.507 x 10 <sup>-3</sup> | 1.073 x 10 <sup>-4</sup>   | 285.419 | 284.421  | 0.0        |
| 4   | -4     | 222.310 | -2.527 x 10 <sup>-1</sup> | -2.527 x 10 <sup>-1</sup> | -3.723 x 10 <sup>-3</sup> | 3.725 x 10 <sup>-4</sup>   | 222.054 | 222.050  | -0.001     |
| 4   | -3     | 224.993 | -1.510 x 10 <sup>-1</sup> | -4.307 x 10 <sup>-3</sup> | 5.960 x 10 <sup>-4</sup>  | -1.547 x 10 <sup>-5</sup>  | 224.839 | 224.844  | 0.0        |
| 4   | -2     | 276.099 | -6.007 x 10 <sup>-1</sup> | -1.163 x 10 <sup>-3</sup> | 8.192 x 10 <sup>-4</sup>  | -2.117 x 10 <sup>-5</sup>  | 275.498 | 275.494  | 00.0       |
| 4   | -1     | 300.919 | -5.565 x 10 <sup>-1</sup> | -8.564 x 10 <sup>-4</sup> | 8.358 x 10 <sup>-4</sup>  | -5.205 x 10 <sup>-5</sup>  | 300.362 | 300.367  | 0.0        |
| 4   | 0      | 316.579 | -8.406 x 10 <sup>-1</sup> | 6.995 x 10 <sup>-3</sup>  | 4.874 x 10 <sup>-4</sup>  | -4.334 x 10 <sup>-5</sup>  | 315.777 | 315.777  | 0.0        |
| 4   | +1     | 384.584 | -2.141 x 10 <sup>0</sup>  | 6.756 x 10 <sup>-2</sup>  | -4.041 x 10 <sup>-3</sup> | 1.179 x 10 <sup>-4</sup>   | 382.517 | 382.520  | 0.0        |
| 4   | +2     | 385.919 | -2.141                    | 6.937 x 10 <sup>-2</sup>  | -4.283 x 10 <sup>-3</sup> | 1.236 x 10 <sup>-4</sup>   | 383.844 | 383.837  | 0.0        |
| 4   | +3     | 494.687 | -6.970                    | 4.234 x 10 <sup>-1</sup>  | -3.471 x 10 <sup>-2</sup> | 1.873 x 10 <sup>-3</sup>   | 488.107 | 488.110  | 0.0        |
| 4   | +4     | 494.712 | -6.969                    | 4.235 x 10 <sup>-1</sup>  | -3.474 x 10 <sup>-2</sup> | 1.874 x 10 <sup>-3</sup>   | 488.133 | 488.133  | +0.001     |
| 5   | -5     | 325.788 | -4.311 x 10 <sup>-1</sup> | -8.251 x 10 <sup>-3</sup> | 1.114 x 10 <sup>-3</sup>  | -4.261 x 10 <sup>-5</sup>  | 325.350 | 325.399  | -0.002     |
| 5   | -4     | 326.971 | -3.370 x 10 <sup>-1</sup> | -9.346 x 10 <sup>-3</sup> | 1.495 x 10 <sup>-3</sup>  | -4.619 x 10 <sup>-5</sup>  | 326.626 | 326.620  | 0.0        |
| 5   | -3     | 400.669 | -1.209                    | -3.695 x 10 <sup>-3</sup> | 2.456 x 10 <sup>-3</sup>  | -9.594 x 10 <sup>-5</sup>  | 399.459 | 399.507  | 0.0        |
| 5   | -2     | 417.118 | -9.005 x 10 <sup>-1</sup> | -1.238 x 10 <sup>-2</sup> | 3.713 x 10 <sup>-3</sup>  | -2.005 x 10 <sup>-4</sup>  | 416.202 | 416.202  | 0.0        |
| 5   | -1     | 448.098 | -1.601                    | 9.379 x 10 <sup>-3</sup>  | 2.799 x 10 <sup>-3</sup>  | -1.654 x 10 <sup>-4</sup>  | 446.510 | 446.560  | +0.001     |
| 5   | 0      | 506.274 | -2.354                    | 5.052 x 10 <sup>-2</sup>  | -7.468 x 10 <sup>-4</sup> | -2.359 x 10 <sup>-4</sup>  | 503.970 | 503.962  | -0.002     |
| 5   | +1     | 511.233 | -2.478                    | 5.960 x 10 <sup>-2</sup>  | -1.726 x 10 <sup>-3</sup> | -1.965 x 10 <sup>-4</sup>  | 508.812 | 508.861  | 0.0        |
| 5   | +2     | 616.482 | -6.723                    | 3.945 x 10 <sup>-1</sup>  | -3.718 x 10 <sup>-2</sup> | 2.021 x 10 <sup>-3</sup>   | 610.115 | 610.101  | 0.0        |
| 5   | +3     | 616.706 | -6.724                    | 3.951 x 10 <sup>-1</sup>  | -3.738 x 10 <sup>-2</sup> | 2.029 x 10 <sup>-3</sup>   | 610.341 | 610.384  | +0.001     |
| 5   | +4     | 757.730 | -17.094                   | 1.625                     | -2.071 x 10 <sup>-1</sup> | 1.732 x 10 <sup>-2</sup>   | 742.072 | 742.107  | +0.001     |
| 5   | +5     | 757.773 | -17.094                   | 1.625                     | -2.072 x 10 <sup>-1</sup> | 1.732 x 10 <sup>-2</sup>   | 742.075 | 742.117  | +0.001     |

Table 9 (Continued)

| $J$ | $\tau$ | $E_R$    | $E_4$                     | $E_6$                     | $E_8$                     | $E_{10}$                  | $E_T$    | Observed | $\Delta E$ |
|-----|--------|----------|---------------------------|---------------------------|---------------------------|---------------------------|----------|----------|------------|
| 6   | -6     | 447.412  | -6.983 x 10 <sup>-1</sup> | -1.558 x 10 <sup>-2</sup> | 2.680 x 10 <sup>-3</sup>  | -1.266 x 10 <sup>-4</sup> | 446.701  | 446.704  | -0.004     |
| 6   | -5     | 447.896  | -6.289 x 10 <sup>-1</sup> | -1.683 x 10 <sup>-2</sup> | 3.113 x 10 <sup>-3</sup>  | -1.240 x 10 <sup>-4</sup> | 447.254  | 447.302  | -0.002     |
| 6   | -4     | 544.915  | -1.998                    | -1.213 x 10 <sup>-2</sup> | 6.459 x 10 <sup>-3</sup>  | -3.365 x 10 <sup>-4</sup> | 542.911  | 542.891  | -0.004     |
| 6   | -3     | 554.438  | -1.504                    | -3.135 x 10 <sup>-2</sup> | 9.520 x 10 <sup>-3</sup>  | -5.388 x 10 <sup>-4</sup> | 552.911  | 552.960  | 0.0        |
| 6   | -2     | 605.741  | -2.997                    | 1.868 x 10 <sup>-2</sup>  | 7.842 x 10 <sup>-3</sup>  | 4.658 x 10 <sup>-4</sup>  | 602.770  | 602.762  | +0.003     |
| 6   | -1     | 651.970  | -3.020                    | 2.170 x 10 <sup>-2</sup>  | 8.985 x 10 <sup>-3</sup>  | -1.162 x 10 <sup>-3</sup> | 648.979  | 649.027  | +0.001     |
| 6   | 0      | 665.044  | -3.559                    | 5.556 x 10 <sup>-2</sup>  | 5.698 x 10 <sup>-3</sup>  | -9.554 x 10 <sup>-4</sup> | 661.546  | 661.534  | +0.002     |
| 6   | +1     | 763.326  | -6.911                    | 3.424 x 10 <sup>-1</sup>  | -2.876 x 10 <sup>-2</sup> | 4.227 x 10 <sup>-4</sup>  | 756.729  | 756.765  | -0.004     |
| 6   | +2     | 764.400  | -6.933                    | 3.467 x 10 <sup>-1</sup>  | -2.976 x 10 <sup>-2</sup> | 4.761 x 10 <sup>-4</sup>  | 757.780  | 757.780  | -0.004     |
| 6   | +3     | 903.766  | -16.508                   | 1.536                     | -2.134 x 10 <sup>-1</sup> | 1.833 x 10 <sup>-2</sup>  | 888.599  | 888.650  | +0.002     |
| 6   | +4     | 903.798  | -16.507                   | 1.537                     | -2.135 x 10 <sup>-1</sup> | 1.833 x 10 <sup>-2</sup>  | 888.634  | 888.592  | +0.001     |
| 6   | +5     | 1076.529 | -35.560                   | 4.873                     | -8.923 x 10 <sup>-1</sup> | 1.068 x 10 <sup>-1</sup>  | 1045.057 | 1045.032 | +0.003     |
| 7   | -7     | 587.369  | -1.098                    | -2.579 x 10 <sup>-2</sup> | 5.396 x 10 <sup>-3</sup>  | -3.041 x 10 <sup>-4</sup> | 586.251  | 586.295  | -0.007     |
| 7   | -6     | 587.560  | -1.054                    | -2.692 x 10 <sup>-2</sup> | 5.784 x 10 <sup>-3</sup>  | -2.966 x 10 <sup>-4</sup> | 586.483  | 586.464  | -0.004     |
| 7   | -5     | 707.161  | -2.911                    | -3.415 x 10 <sup>-2</sup> | 1.521 x 10 <sup>-2</sup>  | -1.058 x 10 <sup>-3</sup> | 704.230  | 704.230  | -0.014     |
| 7   | -4     | 712.041  | -2.390                    | -5.994 x 10 <sup>-2</sup> | 1.972 x 10 <sup>-2</sup>  | -1.285 x 10 <sup>-3</sup> | 709.609  | 709.595  | -0.001     |
| 7   | -3     | 787.385  | -5.033                    | 3.548 x 10 <sup>-2</sup>  | 1.834 x 10 <sup>-2</sup>  | -1.317 x 10 <sup>-3</sup> | 782.405  | 782.455  | -0.006     |
| 7   | -2     | 820.943  | -4.260                    | -1.974 x 10 <sup>-2</sup> | 2.842 x 10 <sup>-2</sup>  | -3.050 x 10 <sup>-3</sup> | 816.689  | 816.670  | +0.003     |
| 7   | -1     | 847.988  | -5.739                    | 7.665 x 10 <sup>-2</sup>  | 1.953 x 10 <sup>-2</sup>  | -2.324 x 10 <sup>-3</sup> | 842.343  | 842.394  | +0.012     |
| 7   | 0      | 935.276  | -7.787                    | 3.676 x 10 <sup>-1</sup>  | -3.344 x 10 <sup>-3</sup> | -3.675 x 10 <sup>-3</sup> | 927.749  | 927.771  | -0.007     |
| 7   | +1     | 938.943  | -7.980                    | 2.897 x 10 <sup>-1</sup>  | -7.327 x 10 <sup>-3</sup> | -3.340 x 10 <sup>-3</sup> | 931.242  | 931.272  | -0.006     |
| 7   | +2     | 1074.923 | -16.482                   | 1.396                     | -1.930 x 10 <sup>-1</sup> | 1.269 x 10 <sup>-2</sup>  | 1059.656 | 1059.632 | -0.007     |
| 7   | +3     | 1075.109 | -16.481                   | 1.398                     | 1.936 x 10 <sup>-1</sup>  | 1.273 x 10 <sup>-2</sup>  | 1059.845 | 1059.900 | -0.007     |
| 7   | +4     | 1246.765 | -34.439                   | 4.654                     | -0.031 x 10 <sup>-1</sup> | 1.117 x 10 <sup>-1</sup>  | 1216.189 | 1216.164 | +0.009     |
| 7   | +5     | 1246.769 | -34.438                   | 4.654                     | -9.031 x 10 <sup>-1</sup> | 1.117 x 10 <sup>-1</sup>  | 1216.194 | 1216.257 | +0.008     |
| 7   | +6     | 1451.090 | -66.038                   | 12.326                    | -3.068                    | 4.976 x 10 <sup>-1</sup>  | 1394.807 | 1394.802 | +0.009     |
| 7   | +7     | 1451.090 | -66.038                   | 12.326                    | -3.068                    | 4.976 x 10 <sup>-1</sup>  | 1394.807 | 1394.881 | +0.009     |
| 8   | -8     | 745.78   | -1.67                     | -3.83 x 10 <sup>-2</sup>  | 9.55 x 10 <sup>-3</sup>   | -6.44 x 10 <sup>-4</sup>  | 744.08   | 744.09   | -0.02      |
| 8   | -7     | 745.85   | -1.65                     | -3.92 x 10 <sup>-2</sup>  | 9.85 x 10 <sup>-3</sup>   | -6.35 x 10 <sup>-4</sup>  | 744.17   | 744.14   | -0.01      |
| 8   | -6     | 886.96   | -3.99                     | -7.52 x 10 <sup>-2</sup>  | 3.13 x 10 <sup>-2</sup>   | -2.67 x 10 <sup>-3</sup>  | 882.92   | 882.97   | -0.03      |
| 8   | -5     | 889.24   | -3.56                     | -1.02 x 10 <sup>-2</sup>  | 3.63 x 10 <sup>-2</sup>   | -2.85 x 10 <sup>-3</sup>  | 885.61   | 885.64   | -0.01      |
| 8   | -4     | 990.41   | -7.575                    | 4.55 x 10 <sup>-2</sup>   | 4.04 x 10 <sup>-2</sup>   | 3.78 x 10 <sup>-3</sup>   | 982.92   | 983.09   | -0.01      |
| 8   | -3     | 1012.27  | -6.14                     | 7.60 x 10 <sup>-2</sup>   | 6.20 x 10 <sup>-2</sup>   | -6.72 x 10 <sup>-3</sup>  | 1006.10  | 1006.14  | +0.01      |
| 8   | -2     | 1059.17  | -9.23                     | -1.43 x 10 <sup>-1</sup>  | 4.31 x 10 <sup>-2</sup>   | -4.95 x 10 <sup>-3</sup>  | 1050.01  | 1050.20  | +0.14      |
| 8   | -1     | 1132.11  | -9.61                     | 1.75 x 10 <sup>-1</sup>   | 4.65 x 10 <sup>-2</sup>   | 1.14 x 10 <sup>-2</sup>   | 1122.27  | 1122.78  | +0.43      |

Table 9 (Continued)

| $J$ | $\tau$ | $E_R$    | $E_4$    | $E_6$                  | $E_8$                   | $E_{10}$                | $E_T$   | Observed | $\Delta E$ |
|-----|--------|----------|----------|------------------------|-------------------------|-------------------------|---------|----------|------------|
| 8   | 0      | 1419.09  | -10.430  | 0.2615                 | $3.302 \times 10^{-2}$  | $-9.846 \times 10^{-3}$ | 1131.76 | 1131.88  | +0.01      |
| 8   | +1     | 1271.47  | -17.36   | 1.21                   | $-1.33 \times 10^{-1}$  | $-1.67 \times 10^{-3}$  | 1255.79 | 1255.19  | +0.12      |
| 8   | +2     | 1272.24  | -17.39   | 1.21                   | $-1.36 \times 10^{-1}$  | $-1.67 \times 10^{-3}$  | 1255.93 | 1255.98  | +0.02      |
| 8   | +3     | 1442.06  | -34.01   | 4.33                   | $8.55 \times 10^{-1}$   | $9.53 \times 10^{-2}$   | 1411.63 | 1311.59  | -0.02      |
| 8   | +4     | 1442.09  | -34.009  | 4.333                  | $=8.550 \times 10^{-1}$ | $9.531 \times 10^{-2}$  | 1411.66 | 1411.59  | -0.02      |
| 8   | +5     | 1645.54  | -64.15   | 11.86                  | -3.08                   | $5.16 \times 10^{-1}$   | 1590.68 | 1590.70  | +0.02      |
| 8   | +6     | 1645.53  | -64.15   | 11.86                  | -3.08                   | $5.16 \times 10^{-1}$   | 1590.68 | 1590.70  | +0.02      |
| 8   | +7     | 1881.412 | -112.867 | 27.529                 | -8.942                  | 1.888                   | 1789.02 | 1789.09  | +0.02      |
| 8   | +8     | 1881.412 | -112.867 | 27.529                 | -8.942                  | 1.888                   | 1789.02 | 1789.09  | +0.02      |
| 9   | -9     | 922.70   | -2.47    | $-5.22 \times 10^{-2}$ | $1.54 \times 10^{-2}$   | $-1.25 \times 10^{-3}$  | 920.19  | 9920.20  | -0.02      |
| 9   | -8     | 922.73   | -2.46    | $-5.28 \times 10^{-2}$ | $1.56 \times 10^{-2}$   | $-1.24 \times 10^{-3}$  | 920.23  | 920.22   | -0.02      |
| 9   | -7     | 1084.55  | -5.33    | $-1.37 \times 10^{-1}$ | $5.70 \times 10^{-2}$   | $-5.77 \times 10^{-3}$  | 1079.13 | 1079.16  | -0.05      |
| 9   | -6     | 1085.55  | -5.04    | $-1.59 \times 10^{-1}$ | $6.14 \times 10^{-2}$   | $-5.85 \times 10^{-3}$  | 1080.41 | 1080.51  | -0.04      |
| 9   | -5     | 1212.26  | -10.39   | $1.55 \times 10^{-2}$  | $8.47 \times 10^{-2}$   | $-1.00 \times 10^{-2}$  | 1201.96 | 1202.04  | -0.04      |
| 9   | -4     | 1224.95  | -8.69    | $-1.54 \times 10^{-1}$ | $1.16 \times 10^{-1}$   | $-1.38 \times 10^{-2}$  | 1216.21 | 1216.37  | +0.02      |
| 9   | -3     | 1296.58  | -14.04   | $2.62 \times 10^{-1}$  | $8.48 \times 10^{-2}$   | $-1.08 \times 10^{-2}$  | 1282.88 | 1283.02  | +0.04      |
| 9   | -2     | 1353.33  | -12.59   | $7.11 \times 10^{-2}$  | $13.0 \times 10^{-1}$   | $-2.49 \times 10^{-2}$  | 1340.86 | 1341.03  | -0.02      |
| 9   | -1     | 1374.70  | -14.92   | $3.28 \times 10^{-1}$  | $9.29 \times 10^{-2}$   | $-1.96 \times 10^{-2}$  | 1360.18 | 1360.56  | +0.05      |
| 9   | 0      | 1493.58  | -19.51   | 9.82                   | $-1.94 \times 10^{-2}$  | $-2.85 \times 10^{-2}$  | 1475.0  | 1475.14  | -0.03      |
| 9   | +1     | 1496.11  | -19.75   | 1.02                   | $-2.99 \times 10^{-1}$  | $-2.70 \times 10^{-2}$  | 1477.73 | 1477.46  | -0.44      |
| 9   | +2     | 1662.72  | -34.67   | 3.91                   | $-7.23 \times 10^{-1}$  | $5.13 \times 10^{-2}$   | 1631.08 | 1631.44  | -0.04      |
| 9   | +3     | 1662.85  | -34.69   | 3.91                   | $-7.24 \times 10^{-1}$  | $5.12 \times 10^{-2}$   | 1631.42 | 1631.58  | -0.04      |
| 9   | +4     | 1864.97  | -63.09   | 11.21                  | -2.97                   | $4.76 \times 10^{-1}$   | 1810.59 | 1810.76  | 0.0        |
| 9   | +5     | 1864.97  | -64.09   | 11.21                  | -2.97                   | $4.76 \times 10^{-1}$   | 1810.59 | 1810.76  | +0.01      |
| 9   | +6     | 2100.06  | -199.93  | 26.63                  | -8.93                   | 1.95                    | 2009.78 | 2010.0   | +0.05      |
| 9   | +7     | 2100.06  | -199.93  | 26.63                  | -8.93                   | 1.95                    | 2009.78 | 2010.0   | +0.05      |
| 9   | +8     | 2367.50  | -181.06  | 55.91                  | -22.97                  | 6.12                    | 2225.50 | 2225.6   | +0.03      |
| 9   | +9     | 2367.50  | -181.06  | 55.91                  | -22.97                  | 6.12                    | 2225.50 | 2225.6   | +0.03      |
| 10  | -10    | 1118.16  | -3.54    | $-6.54 \times 10^{-2}$ | $2.29 \times 10^{-2}$   | $-2.27 \times 10^{-3}$  | 1114.57 | 1114.59  | -0.04      |
| 10  | -9     | 1118.17  | -3.54    | $-6.57 \times 10^{-2}$ | $2.30 \times 10^{-2}$   | $-2.26 \times 10^{-3}$  | 1114.59 | 1114.59  | -0.09      |
| 10  | -8     | 1300.26  | -6.84    | $-2.32 \times 10^{-1}$ | $9.75 \times 10^{-2}$   | $-1.13 \times 10^{-2}$  | 1293.10 | 1203.22  | -0.08      |
| 10  | -7     | 1300.67  | -7.02    | $-2.18 \times 10^{-1}$ | $9.40 \times 10^{-2}$   | $-1.12 \times 10^{-2}$  | 1293.68 | 1293.80  | -0.04      |
| 10  | -6     | 1451.42  | -13.42   | $-8.68 \times 10^{-2}$ | $1.64 \times 10^{-1}$   | $-2.32 \times 10^{-2}$  | 1438.06 | 1438.19  | -0.09      |
| 10  | -5     | 1458.07  | -11.86   | $-2.66 \times 10^{-1}$ | $1.98 \times 10^{-1}$   | $2.70 \times 10^{-2}$   | 1446.11 | 1446.23  | +0.01      |
| 10  | -4     | 1557.54  | -19.95   | $4.07 \times 10^{-1}$  | $1.63 \times 10^{-1}$   | $-2.40 \times 10^{-2}$  | 1538.14 | 1538.31  | +0.02      |

Table 9 (Continued)

| $J$ | $\tau$ | $E_R$   | $E_4$   | $E_6$                    | $E_8$                    | $E_{10}$                 | $E_{12}$ | Observed | $\Delta E$ |
|-----|--------|---------|---------|--------------------------|--------------------------|--------------------------|----------|----------|------------|
| 10  | -3     | 1597.94 | -16.83  | -4.30 x 10 <sup>-2</sup> | 2.61 x 10 <sup>-1</sup>  | -4.83 x 10 <sup>-2</sup> | 1581.28  | 1581.53  | +0.35      |
| 10  | -2     | 1451.43 | -13.42  | -8.68 x 10 <sup>-2</sup> | 1.64 x 10 <sup>-1</sup>  | -2.32 x 10 <sup>-2</sup> | 1616.34  | 1616.49  | +0.12      |
| 10  | -1     | 1741.21 | -23.38  | 7.46 x 10 <sup>-1</sup>  | 1.66 x 10 <sup>-1</sup>  | -7.17 x 10 <sup>-2</sup> | 1718.72  | 1719.36  | +0.01      |
| 10  | 0      | 1748.04 | -24.34  | 9.06 x 10 <sup>-1</sup>  | 1.31 x 10 <sup>-1</sup>  | -6.52 x 10 <sup>-2</sup> | 1724.68  | 1724.80  | +0.02      |
| 10  | +1     | 1909.01 | -36.88  | 3.40                     | -4.79 x 10 <sup>-1</sup> | -2.83 x 10 <sup>-2</sup> | 1875.03  | 1875.24  | -0.07      |
| 10  | +2     | 1909.53 | -36.92  | 3.41                     | -4.85 x 10 <sup>-1</sup> | -2.75 x 10 <sup>-2</sup> | 1875.52  | 1875.    | +0.03      |
| 10  | +3     | 2109.67 | -63.32  | 10.36                    | -2.69                    | -3.60 x 10 <sup>-1</sup> | 2054.38  | 2054.55  | -0.02      |
| 10  | +4     | 2109.67 | 63.32   | 10.36                    | -2.69                    | -3.60 x 10 <sup>-1</sup> | 2054.38  | 2054.55  | -0.02      |
| 10  | +5     | 2343.67 | -107.99 | 25.42                    | -8.70                    | 1.86                     | 2254.3   | 2254.5   | 0.0        |
| 10  | +6     | 2343.67 | -107.99 | 25.42                    | -8.70                    | 1.86                     | 2254.3   | 2254.5   | 0.0        |
| 10  | +7     | 2610.37 | -176.75 | 54.32                    | -22.90                   | 6.30                     | 2471.32  | 2471.6   | +0.07      |
| 10  | +8     | 2610.37 | -176.75 | 54.32                    | -22.90                   | 6.30                     | 2471.32  | 2571.6   | 0.07       |
| 10  | +9     | 2909.3  | -376.3  | 10.54                    | -5.34                    | 1.75                     | 2702.52  | 2702.1   | +0.03      |
| 10  | +10    | 2909.3  | -276.3  | 10.54                    | -5.34                    | 1.75                     | 2702.52  | 2702.9   | +0.03      |



Table 10

CONTRIBUTION TO TOTAL ROTATIONAL  
ENERGY OF VARIOUS TERMS OF THE HAMILTONIAN

| $J$ | $\tau$ | $E_R$   | $E_4$    | $E_6$  | $E_8$   | $E_{10}$ | $E_T$   | Observed |
|-----|--------|---------|----------|--------|---------|----------|---------|----------|
| 11  | 11     | 3506.95 | -404.92  | 186.86 | -114.63 | 45.46    | 3219.71 | 3216.6   |
| 11  | 10     | 3506.95 | -404.92  | 186.86 | -114.63 | 45.46    | 3219.71 | 3216.6   |
| 11  | 9      | 317.43  | -270.26  | 102.69 | -53.19  | 17.99    | 2973.65 | 2973.07  |
| 11  | 8      | 3176.43 | -270.26  | 102.69 | -53.19  | 17.99    | 2973.65 | 2973.07  |
| 11  | 7      | 2878.15 | -173.62  | 52.22  | -22.41  | 6.13     | 2740.47 | 2740.73  |
| 11  | 6      | 2878.15 | -173.62  | 52.22  | -22.41  | 6.13     | 2740.47 | 2740.73  |
| 11  | 5      | 2612.45 | -107.53  | 23.89  | -8.15   | 1.59     | 2522.25 | 2522.46  |
| 11  | 4      | 2612.45 | -107.53  | 23.89  | -8.15   | 1.59     | 2522.25 | 2522.46  |
|     |        |         |          |        |         |          |         |          |
| 12  | 12     | 4160.32 | -573.97  | 315.26 | -230.13 | 108.43   | 3779.92 | 3767.1   |
| 12  | 11     | 4160.32 | -573.97  | 315.26 | -230.13 | 108.43   | 3779.92 | 3767.1   |
| 12  | 10     | 3798.26 | -396.77  | 182.62 | -114.07 | 46.51    | 3516.56 | 3512.8   |
| 12  | 9      | 3798.26 | -396.77  | 182.62 | -114.07 | 46.51    | 3516.56 | 3512.8   |
| 12  | 8      | 3468.41 | -265.59  | 99.29  | -52.25  | 17.72    | 3267.56 | 3267.2   |
| 12  | 7      | 3468.41 | -265.59  | 99.29  | -52.25  | 17.72    | 3267.56 | 3267.2   |
| 12  | 6      | 3171.04 | -172.18  | 49.83  | -21.38  | 5.55     | 3032.65 | 3033.17  |
| 12  | 5      | 3171.04 | -172.18  | 49.83  | -21.38  | 5.55     | 3032.65 | 3033.17  |
| 12  | 4      | 2906.64 | -109.09  | 22.05  | -7.21   | 1.09     | 2813.48 | 2813.94  |
| 12  | 3      | 2906.64 | -109.09  | 22.05  | -7.21   | 1.09     | 2813.48 | 2813.94  |
|     |        |         |          |        |         |          |         |          |
| 13  | 13     | 4869.44 | -791.13  | 510.03 | -436.87 | 241.28   | 4392.76 | --       |
| 13  | 12     | 4869.44 | -791.13  | 510.03 | -436.87 | 241.28   | 4392.76 | --       |
| 13  | 11     | 4475.86 | -563.24  | 308.78 | -228.93 | 107.55   | 4103.21 | --       |
| 13  | 10     | 4465.86 | -563.24  | 308.78 | -228.93 | 107.55   | 4103.21 | --       |
| 13  | 9      | 4114.44 | -390.17  | 177.31 | -112.33 | 46.13    | 3835.38 | --       |
| 13  | 8      | 4114.44 | -390.17  | 177.31 | -112.33 | 46.13    | 3835.38 | --       |
| 13  | 7      | 3785.43 | -262.84  | 95.11  | -50.40  | 16.57    | 3584.0  | 3583.87  |
| 13  | 6      | 3785.43 | -262.84  | 95.11  | -50.40  | 16.57    | 3584.0  | 3583.87  |
| 13  | 5      | 3489.24 | -173.02  | 46.52  | -19.68  | 4.47     | 3347.52 | 3348.2   |
| 13  | 4      | 3489.24 | -173.02  | 46.52  | -19.68  | 4.47     | 3347.52 | 3348.2   |
|     |        |         |          |        |         |          |         |          |
| 14  | 14     | 5645.45 | -1064.77 | 796.17 | -790.83 | 506.0    | 5080.91 | --       |
| 14  | 13     | 5634.34 | -1064.77 | 796.17 | -790.83 | 506.0    | 5080.91 | --       |
| 14  | 12     | 5209.21 | -777.36  | 500.45 | -434.58 | 246.08   | 4743.81 | --       |
| 14  | 11     | 5209.21 | -777.36  | 500.45 | -434.58 | 246.08   | 4743.81 | --       |
| 14  | 10     | 4816.24 | -554.30  | 300.80 | -225.88 | 110.36   | 4447.22 | --       |
| 14  | 9      | 4816.24 | -554.30  | 300.80 | -225.88 | 110.36   | 4447.22 | --       |
| 14  | 8      | 4455.63 | -385.24  | 170.88 | -109.13 | 44.04    | 4175.67 | --       |
| 14  | 7      | 4455.63 | -385.24  | 170.88 | -109.13 | 44.04    | 4175.67 | --       |
| 14  | 6      | 4127.69 | -262.64  | 90.14  | -47.42  | 14.40    | 3922.17 | --       |
| 14  | 5      | 4127.69 | -262.64  | 90.14  | -47.42  | 14.40    | 3922.17 | --       |
| 14  | 4      | 3832.98 | -176.80  | 42.95  | -17.14  | 2.80     | 3684.78 | --       |
| 14  | 3      | 3832.97 | -176.80  | 42.95  | -17.14  | 2.80     | 3684.47 | --       |

Table 10 (Continued)

| $J$ | $\tau$ | $E_R$   | $E_4$    | $E_6$   | $E_8$    | $E_{10}$ | $E_T$   | Observed |
|-----|--------|---------|----------|---------|----------|----------|---------|----------|
| 15  | 15     | 6454.99 | -1403.93 | 1205.16 | -3174.06 | 1008.29  | 5890.05 | --       |
| 15  | 14     | 6454.99 | -1403.93 | 1205.16 | -1324.06 | 1008.29  | 5890.05 | --       |
| 15  | 13     | 5998.33 | -1047.42 | 782.41  | -786.72  | 515.43   | 5462.03 | --       |
| 15  | 12     | 5998.33 | -1047.42 | 782.41  | -786.72  | 515.43   | 5462.03 | --       |
| 15  | 11     | 5573.81 | -765.58  | 488.83  | -429.43  | 245.97   | 5113.59 | --       |
| 15  | 10     | 5573.58 | -765.58  | 488.83  | -429.43  | 245.97   | 5113.59 | --       |
| 15  | 9      | 5181.60 | -547.77  | 291.24  | -220.53  | 106.75   | 4811.28 | --       |
| 15  | 8      | 5181.60 | -547.77  | 291.24  | -220.53  | 106.75   | 4811.28 | --       |
| 15  | 7      | 4821.98 | -384.14  | 163.28  | -104.13  | 39.93    | 4536.93 | --       |
| 15  | 6      | 4821.98 | -384.14  | 163.28  | -104.13  | 39.93    | 4536.93 | --       |
| 15  | 5      | 4495.38 | -265.69  | 84.43   | -43.08   | 11.02    | 4282.06 | --       |
| 15  | 4      | 4495.38 | -265.69  | 84.43   | -43.08   | 11.02    | 4282.06 | --       |
| 15  | 3      | 4202.53 | -184.29  | 39.03   | -13.61   | 4.31     | 4044.10 | 4045.8   |
| 15  | 2      | 4202.50 | -184.28  | 39.03   | -13.61   | 4.30     | 4044.06 | 4045.8   |
| 15  | 1      | 3945.04 | -132.88  | 15.57   | -1.13    | -2.25    | 3824.35 | 2836.1   |
| 15  | 0      | 3944.38 | -132.65  | 15.48   | -1.08    | -2.27    | 3823.86 | 3824.8   |
| 15  | -1     | 3728.41 | -106.86  | 6.24    | 2.75     | -2.05    | 3628.5  | 3628.7   |
| 15  | -2     | 3721.27 | -103.65  | 5.23    | 3.10     | -2.20    | 2623.75 | 3624.0   |
| 15  | -3     | 3568.22 | -103.60  | 5.88    | 2.69     | -1.19    | 3472.0  | 3473.0   |
| 16  | 16     | 7331.41 | -1818.30 | 1775.99 | -2303.69 | 1921.77  | 6907.18 | --       |
| 16  | 15     | 7331.41 | -1818.30 | 1775.99 | -2303.69 | 1921.77  | 6907.18 | --       |
| 16  | 14     | 6843.21 | -382.43  | 1185.89 | -367.08  | 1025.98  | 6305.57 | --       |
| 16  | 13     | 6843.21 | -1382.43 | 1185.89 | -1367.08 | 1025.98  | 6305.37 | --       |
| 16  | 12     | 6387.14 | -1032.31 | 765.93  | -778.33  | 516.30   | 5858.73 | --       |
| 16  | 11     | 6387.14 | -1032.31 | 765.93  | -778.33  | 516.30   | 5858.73 | --       |
| 16  | 10     | 5963.35 | -756.50  | 475.03  | -420.79  | 240.09   | 5501.19 | --       |
| 16  | 9      | 5963.35 | -756.50  | 475.03  | -420.79  | 240.09   | 5501.19 | --       |
| 16  | 8      | 5572.08 | -544.36  | 280.05  | -212.41  | 99.40    | 5194.75 | --       |
| 16  | 7      | 5572.08 | -544.36  | 280.05  | -212.41  | 99.40    | 5194.75 | --       |
| 16  | 6      | 5213.68 | -386.10  | 154.57  | -96.98   | 33.49    | 4918.66 | --       |
| 16  | 5      | 5213.68 | -386.10  | 154.57  | -96.98   | 33.49    | 4918.66 | --       |
| 16  | 4      | 4888.72 | -272.77  | 78.09   | -37.13   | 6.23     | 4663.14 | --       |
| 16  | 3      | 4888.72 | -272.77  | 78.09   | -37.13   | 6.23     | 4663.14 | --       |
| 16  | 2      | 4598.22 | -196.35  | 34.98   | -8.93    | -2.76    | 4425.15 | --       |
| 16  | 1      | 4598.09 | -196.31  | 34.96   | -8.92    | -2.77    | 4425.05 | --       |
| 16  | 0      | 4344.76 | -150.33  | 13.88   | 2.25     | -4.18    | 4206.39 | --       |
| 16  | -1     | 4342.94 | -149.43  | 13.53   | 2.42     | -4.26    | 4205.20 | --       |
| 16  | -2     | 4137.73 | -132.16  | 7.65    | 4.73     | -3.02    | 4014.93 | --       |
| 16  | -3     | 4122.07 | -123.83  | 4.86    | 5.67     | -3.46    | 4005.30 | --       |
| 16  | -4     | 3992.13 | -134.13  | 9.35    | 3.82     | -1.72    | 3869.44 | --       |
| 16  | -5     | 3924.18 | -107.31  | 1.52    | 5.79     | -2.51    | 3821.67 | --       |
| 16  | -6     | 3874.30 | -124.67  | 7.53    | 3.78     | -1.52    | 3759.41 | --       |

Table 10 (Continued)

| $J$ | $\tau$ | $E_R$   | $E_4$  | $E_6$ | $E_8$ | $E_{10}$ | $E_T$   | Observed |
|-----|--------|---------|--------|-------|-------|----------|---------|----------|
| 16  | -7     | 3725.71 | -88.54 | -0.92 | 4.92  | -1.83    | 3639.34 | 3657.1   |
| 16  | -8     | 3716.63 | -95.31 | 1.15  | 4.31  | -1.63    | 3625.16 | 3640.3   |
| 16  | -9     | 3505.84 | -66.01 | -2.62 | 3.46  | -1.20    | 3439.47 | 3439.7   |
| 16  | -10    | 3505.01 | -67.00 | -2.36 | 3.39  | -1.18    | 3437.86 | 3437.7   |

From the work in chapter 3, expectations are that due to the strong coupling between the vibrational and rotational motions, the various coefficients in equation (5.3) will exhibit a strong dependence on whichever set of states is used for fitting purposes. In these calculations, the fit is to energy levels instead of spectral lines. Although there are far more spectral lines than levels, both sets of data contain exactly the same information on the physical structure of the system. Owing to the large number of lines, the standard deviations obtained in a least squares analysis will be much smaller than that obtained from fits to energy levels. However, since the additional equations can all be obtained from those equations used to fit to energies, it is unlikely that the value of the rotation constants, etc., would change significantly. Furthermore, the coefficients derived from spectral lines will be much more strongly correlated than those derived from an energy level analysis and, consequently, less reliable.

In table 11, the coefficients that arise from a least squares analysis of high  $\tau$  states are compared to those derived from low  $\tau$  states. More precisely, the following 68 levels were used for the high  $\tau$  fit:  $5_1-5_5$ ;  $6_1-6_6$ ;  $7_1-7_7$ ;  $8_1-8_8$ ;  $9_1-9_9$ ;  $10_1-10_{10}$  and  $11_1-11_{11}$ . The low  $\tau$  fit used  $1_{-1}, 1_0, 1_1$ ;  $2_{-2}, 2_{-1}$ ;  $3_{-3}, 3_{-1}$ ;  $4_{-4}, 4_{-1}$ ;  $5_{-5}, 5_{-1}$ ;  $6_{-6}, 6_{-1}$ ;  $7_{-7}, 7_{-1}$ ;  $8_{-8}, 8_{-1}$ ;  $9_{-9}, 9_{-1}$ ;  $10_{-10}, 10_{-1}$  and  $11_{-11}, 11_{-1}$ . In both cases, these coefficients yielded energy eigenvalues that deviated by only a few hundredths of a wave number from the measured energy levels used for fitting.

An examination of table 11 reveals that most of the fourth-order and virtually all of the higher order distortion coefficients of the low and high  $\tau$  fits deviate from one another by more than a standard deviation. For example, at the center of their distributions, the high and low  $\tau$   $\Delta_K$  differ by a factor of 2. For  $\delta_J$ , the difference is an order of magnitude and for  $\delta_K$ , two orders of magnitude. Also, there is a sign difference. These deviations are serious because the fourth-order energy is generally large and implies serious errors would be present for any wave function generated from these constants. In general,



the higher order coefficients deviate from one to four orders of magnitude with sign changes. The value of these coefficients is then completely determined by the immediate levels used for fitting and do not reflect the physical structure of the molecule.

The cause of these difficulties lies in the fact that the rotation-vibration energy of the high  $\tau$  states is much greater than that of the low  $\tau$  levels. Since no effort has been made to remove this energy from the distortion coefficients, they strongly reflect its presence. A second difficulty lies in the fact that the separation between the rotational levels (i.e., between different  $\tau$ 's of a fixed  $J$  and a different vibrational band) is now comparable to the vibrational energy splitting. For example, the vibrational energy difference between the ground and first excited bending mode is about  $1600 \text{ cm}^{-1}$ . For the rotational splitting

$$E_{\nu} = 1, J = 9, \tau = 9 - E_{\nu} = 0, J = 9, \tau = 5 \\ - 1600 \text{ cm}^{-1} \approx 800 \text{ cm}^{-1},$$

which is half the vibrational energy difference. These coefficients depend strongly on the energy difference between the rotation-vibration levels that are coupled together by the nonrigid terms of the Hamiltonian. Consequently, they will depend strongly on the structure of the rotational state when the rotational energy splitting becomes comparable to the vibrational spacings.

In table 12, a comparison is made between the high and low  $J$  levels. In particular, a fit was made to 70 levels in the  $J = 1$  to 8 states and to all of the  $J = 10, 11, 12$  states. Deviations again arise in the fourth order, as in the case of high and low  $\tau$ . However, owing to the large standard deviations, less detail can be obtained from this table.

#### PREDICTABILITY

The ability of equation (5.3) to predict the positions of new energy levels has been examined. Specifically a comparison was made of the

predicted rotational levels that arise from the Watson Hamiltonian [i.e., equation (5.3)] for the following sets of rotation-distortion coefficients: (1) low  $\tau$ ; (2) high  $\tau$ ; (3) low  $J$ ; (4) high  $J$ , (5) reference 12. Our results show that serious discrepancies appear in all cases, although reference 12 is far superior to the others.

#### Low $\tau$

First, the results of fitting to the low  $\tau$  states will be discussed. In table 13 are listed the predicted values versus the observed values for the different rotational states through  $J = 16$ . Note that those levels that were chosen for fitting purposes are reproduced to better than  $0.05 \text{ cm}^{-1}$ . First, consider the high  $\tau$  states for  $J \leq 11$ . (Recall that the low  $\tau$  states for  $J \leq 11$  were used for fitting purposes.) An examination of table 13 reveals that deviations on the order of a few tenths of a wave number have already appeared by the  $J = 3$  and 4 states. For the  $5_2$  and  $5_3$  states, deviations of  $2 \text{ cm}^{-1}$  occur; and for the  $5_4$  and  $5_5$  states, there is a discrepancy between theory and experiment of about  $10 \text{ cm}^{-1}$ . Similarly, for the  $6_3$ ,  $6_4$  states, deviations of about  $0.7 \text{ cm}^{-1}$  appear; and for the  $6_5$  and  $6_6$  rotational levels, errors on the order of  $40 \text{ cm}^{-1}$  have appeared. This trend continues, i.e., greater and greater discrepancies between theory and experiment arise in the  $J = 8$  and  $J = 9$  rotational multiplets. Finally, by  $J = 10$ , there is no resemblance between the predicted energies and the observed ones. For example, the  $10_1$  and  $10_2$  states deviate by  $9 \text{ cm}^{-1}$ ; for  $10_7$  and  $10_8$ , the predicted energies are negative, a situation that arose for the case of a rotating Morse oscillator.

Next, consider the low  $\tau$  levels for  $J \geq 12$ . An examination of table 13 reveals that  $12_{-12} - 12_{-2}$  rotational energies are in reasonable agreement with experiment. However, beyond this, the situation rapidly deteriorates. Similarly, the states  $13_{-13} - 13_{-3}$  are fairly well predicted, although the  $13_{-2}$  level deviates by  $15 \text{ cm}^{-1}$  from the experiment. By  $J = 14$ , serious discrepancies arise by  $\tau = -6$ , for  $J = 15$  by  $\tau = -7$ , and for  $J = 16$  by  $\tau = -14$ .

Table 11

TEST FOR UNIQUENESS OF LEAST SQUARES FITTING  
FOR HIGH AND LOW  $\tau$

|               | Low $\tau$   | High $\tau$   |
|---------------|--|---|
| A             | $2.7861234 \times 10^1 \pm 2.1908565 \times 10^{-2}$     | $2.790118 \times 10^1 \pm 1.1406407 \times 10^{-2}$       |
| B             | $1.4521751 \times 10^{-1} \pm 3.8477284 \times 10^{-3}$  | $1.4445913 \times 10^1 \pm 8.1378196 \times 10^{-2}$      |
| C             | $9.2816871 \pm 3.1585214 \times 10^{-3}$                 | $9.3003991 \pm 1.0102989 \times 10^{-1}$                  |
| $\Delta_J$    | $1.2751778 \times 10^{-3} \pm 3.9871204 \times 10^{-5}$  | $-2.1136767 \times 10^{-3} \pm 2.7358925 \times 10^{-3}$  |
| $\Delta_{JK}$ | $-4.2498711 \times 10^{-3} \pm 1.2848932 \times 10^{-3}$ | $-4.6654608 \times 10^{-4} \pm 8.7506809 \times 10^{-3}$  |
| $\Delta_K$    | $1.6380750 \times 10^{-2} \pm 6.9675567 \times 10^{-3}$  | $3.4500498 \times 10^{-2} \pm 5.6726837 \times 10^{-3}$   |
| $\delta_K$    | $4.9866468 \times 10^{-4} \pm 2.3341136 \times 10^{-5}$  | $4.9825552 \times 10^{-3} \pm 2.7474778 \times 10^{-3}$   |
| $\delta_K$    | $1.5422853 \times 10^{-4} \pm 1.3868588 \times 10^{-3}$  | $-5.4694406 \times 10^{-2} \pm 3.5702885 \times 10^{-2}$  |
| $H_J$         | $6.6118469 \times 10^{-7} \pm 2.2555794 \times 10^{-7}$  | $1.5868118 \times 10^{-4} \pm 7.8205148 \times 10^{-5}$   |
| $H_{JK}$      | $2.4312591 \times 10^{-5} \pm 9.3611777 \times 10^{-6}$  | $-2.1034987 \times 10^{-3} \pm 1.0772050 \times 10^{-3}$  |
| $H_{KJ}$      | $2.1972752 \times 10^{-4} \pm 1.5221769 \times 10^{-4}$  | $4.9642308 \times 10^{-3} \pm 2.5955161 \times 10^{-3}$   |
| $H_K$         | $-2.6745956 \times 10^{-3} \pm 1.0754196 \times 10^{-3}$ | $-2.9120505 \times 10^{-3} \pm 1.5904144 \times 10^{-3}$  |
| $h_j$         | $1.7076044 \times 10^{-7} \pm 1.2714262 \times 10^{-7}$  | $-7.6465990 \times 10^{-5} \pm 3.7979067 \times 10^{-5}$  |
| $h_{JK}$      | $7.5151086 \times 10^{-6} \pm 3.7290733 \times 10^{-6}$  | $1.5419958 \times 10^{-3} \pm 7.7448027 \times 10^{-4}$   |
| $h_K$         | $-2.3783418 \times 10^{-4} \pm 2.5585506 \times 10^{-4}$ | $-5.4848512 \times 10^{-3} \pm 2.9108518 \times 10^{-3}$  |
| $L_{JK}$      | $-2.1781492 \times 10^{-6} \pm 7.5333344 \times 10^{-7}$ | $4.2607054 \times 10^{-6} \pm 2.5026737 \times 10^{-6}$   |
| $L_{KJ}$      | $1.4896433 \times 10^{-5} \pm 9.1730935 \times 10^{-6}$  | $-1.1822368 \times 10^{-5} \pm 6.9779067 \times 10^{-6}$  |
| $L_K$         | $7.1554451 \times 10^{-5} \pm 5.6518559 \times 10^{-5}$  | $7.2549200 \times 10^{-6} \pm 4.4860100 \times 10^{-6}$   |
| $l_K$         | $1.7274188 \times 10^{-5} \pm 1.3524660 \times 10^{-5}$  | $8.8590460 \times 10^{-6} \pm 5.4370631 \times 10^{-6}$   |
| $P_K$         | $-1.4597506 \times 10^{-5} \pm 7.5929448 \times 10^{-7}$ | $5.1953952 \times 10^{-10} \pm 1.7756653 \times 10^{-10}$ |
| $p_K$         | $-2.3539468 \times 10^{-7} \pm 2.2110777 \times 10^{-7}$ | $4.5974880 \times 10^{-9} \pm 2.8869232 \times 10^{-9}$   |

Table 12

TEST FOR UNIQUENESS OF LEAST SQUARES FITTING  
FOR  $J = 1-8, 10, 11, 12$

|               | $J = 10, 11, 12$            |                                 | $J = 1-8$                    |                                |
|---------------|-----------------------------|---------------------------------|------------------------------|--------------------------------|
| A             | $2.8021076 \times 10^1$     | $\pm 1.2584273 \times 10^{-1}$  | $2.7877399 \times 10^1$      | $\pm 5.7776983 \times 10^{-3}$ |
| B             | $1.4475654 \times 10^1$     | $\pm 3.8022468 \times 10^{-2}$  | $1.4521195 \times 10^1$      | $\pm 3.5283291 \times 10^{-3}$ |
| C             | 9.2749972                   | $\pm 1.9043611 \times 10^{-2}$  | 9.2772397                    | $\pm 3.1810502 \times 10^{-3}$ |
| $\Delta_J$    | $9.4049653 \times 10^{-4}$  | $\pm 2.4951000 \times 10^{-4}$  | $1.2206764 \times 10^{-3}$   | $\pm 8.5179333 \times 10^{-5}$ |
| $\Delta_{JK}$ | $-4.4687892 \times 10^{-3}$ | $\pm 2.0059901 \times 10^{-3}$  | $-6.0803482 \times 10^{-3}$  | $\pm 5.4899506 \times 10^{-4}$ |
| $\Delta_K$    | $3.5623288 \times 10^{-2}$  | $\pm 2.1873472 \times 10^{-3}$  | $3.2391491 \times 10^{-2}$   | $\pm 9.0682603 \times 10^{-4}$ |
| $\delta_J$    | $3.5035443 \times 10^{-4}$  | $\pm 1.8738260 \times 10^{-4}$  | $5.1759149 \times 10^{-4}$   | $\pm 7.4186159 \times 10^{-5}$ |
| $\delta_k$    | $1.6797911 \times 10^{-3}$  | $\pm 3.3470801 \times 10^{-4}$  | $1.2575220 \times 10^{-3}$   | $\pm 1.2739147 \times 10^{-3}$ |
| $H_J$         | $-3.8357118 \times 10^{-7}$ | $\pm 9.2518603 \times 10^{-7}$  | $5.7229858 \times 10^{-7}$   | $\pm 1.2563280 \times 10^{-6}$ |
| $H_{JK}$      | $-2.5619922 \times 10^{-6}$ | $\pm 7.4562113 \times 10^{-6}$  | $-1.4591014 \times 10^{-5}$  | $\pm 1.6255732 \times 10^{-5}$ |
| $H_{KJ}$      | $1.2740388 \times 10^{-5}$  | $\pm 2.0188034 \times 10^{-5}$  | $-2.7046471 \times 10^{-5}$  | $\pm 4.0917037 \times 10^{-5}$ |
| $H_K$         | $1.3581069 \times 10^{-4}$  | $\pm 2.4762050 \times 10^{-5}$  | $1.4235874 \times 10^{-4}$   | $\pm 5.3898739 \times 10^{-5}$ |
| $h_J$         | $-2.7959194 \times 10^{-7}$ | $\pm 6.9202722 \times 10^{-7}$  | $3.0319408 \times 10^{-7}$   | $\pm 6.7186041 \times 10^{-7}$ |
| $h_{JK}$      | $1.8733722 \times 10^{-7}$  | $\pm 3.5403482 \times 10^{-6}$  | $1.2472925 \times 10^{-5}$   | $\pm 1.9690785 \times 10^{-5}$ |
| $h_K$         | $4.3887342 \times 10^{-5}$  | $\pm 2.2086231 \times 10^{-5}$  | $-6.8265611 \times 10^{-5}$  | $\pm 2.8141018 \times 10^{-4}$ |
| $L_{JK}$      | $-3.5071943 \times 10^{-7}$ | $\pm 2.5076621 \times 10^{-7}$  | $3.1812650 \times 10^{-6}$   | $\pm 4.4365160 \times 10^{-6}$ |
| $L_{KJ}$      | $9.2501065 \times 10^{-7}$  | $\pm 7.5724814 \times 10^{-7}$  | $-8.4370406 \times 10^{-6}$  | $\pm 1.2577229 \times 10^{-5}$ |
| $L_k$         | $-1.1867769 \times 10^{-6}$ | $\pm 5.0924892 \times 10^{-7}$  | $4.9919688 \times 10^{-6}$   | $\pm 8.2803728 \times 10^{-6}$ |
| $\lambda_K$   | $-1.0525886 \times 10^{-6}$ | $\pm 7.1830927 \times 10^{-7}$  | $4.2204533 \times 10^{-6}$   | $\pm 1.2441923 \times 10^{-5}$ |
| $P_K$         | $1.1888523 \times 10^{-9}$  | $\pm 5.1584160 \times 10^{-10}$ | $-3.0137686 \times 10^{-10}$ | $\pm 4.8525514 \times 10^{-9}$ |
| $p_K$         | $6.4596572 \times 10^{-10}$ | $\pm 9.0045005 \times 10^{-10}$ | $3.7693584 \times 10^{-8}$   | $\pm 4.1545549 \times 10^{-8}$ |



Table 13

## PREDICABILITY OF VARIOUS FITS

| $J$ | $\tau$ | Obs.     | Low $\tau$ | High $\tau$ | Low $J$ | High $J$ |
|-----|--------|----------|------------|-------------|---------|----------|
| 1   | 1      | 23.791   | 23.80      | 23.76       | 23.80   | 23.79    |
| 1   | 0      | 37.137   | 37.13      | 37.08       | 37.13   | 37.02    |
| 1   | +1     | 42.362   | 42.37      | 42.39       | 42.37   | 42.26    |
| 2   | -2     | 70.088   | 70.10      | 70.03       | 70.09   | 70.09    |
| 2   | -1     | 79.496   | 79.49      | 79.41       | 79.49   | 79.40    |
| 2   | 0      | 95.174   | 95.17      | 95.16       | 95.18   | 95.08    |
| 2   | 1      | 134.902  | 134.92     | 134.86      | 134.89  | 134.48   |
| 2   | 2      | 136.1611 | 136.18     | 136.19      | 136.16  | 135.75   |
| 3   | -3     | 136.765  | 136.78     | 137.03      | 136.76  | 136.74   |
| 3   | -2     | 142.274  | 142.28     | 142.62      | 142.28  | 142.20   |
| 3   | -1     | 173.370  | 173.37     | 173.21      | 173.38  | 173.29   |
| 3   | 0      | 206.303  | 206.33     | 206.15      | 206.30  | 205.96   |
| 3   | 1      | 212.162  | 212.18     | 212.18      | 212.16  | 211.85   |
| 3   | 2      | 285.217  | 284.90     | 285.21      | 285.21  | 284.37   |
| 3   | 3      | 285.421  | 285.10     | 285.42      | 285.41  | 284.67   |
| 4   | -4     | 222.050  | 222.08     | 224.06      | 222.06  | 222.01   |
| 4   | -3     | 224.844  | 224.84     | 227.05      | 224.84  | 224.77   |
| 4   | -2     | 275.494  | 275.50     | 275.09      | 275.51  | 275.42   |
| 4   | -1     | 300.367  | 300.39     | 300.19      | 300.37  | 300.11   |
| 4   | 0      | 315.777  | 315.81     | 315.68      | 315.79  | 315.57   |
| 4   | 1      | 382.521  | 382.36     | 382.43      | 382.52  | 381.89   |
| 4   | 2      | 383.837  | 383.69     | 383.84      | 383.84  | 383.23   |
| 4   | 3      | 488.110  | 485.55     | 488.12      | 488.12  | 486.84   |
| 4   | 4      | 488.126  | 485.58     | 488.15      | 488.14  | 486.87   |
| 5   | -5     | 325.399  | 325.38     | 332.70      | 325.36  | 325.29   |
| 5   | -4     | 326.620  | 326.62     | 334.25      | 326.64  | 326.56   |
| 5   | -3     | 399.50   | 399.47     | 399.01      | 399.47  | 399.37   |
| 5   | -2     | 416.202  | 426.21     | 416.49      | 416.23  | 416.04   |
| 5   | -1     | 446.56   | 446.53     | 445.93      | 446.53  | 446.38   |
| 5   | 0      | 593.961  | 593.92     | 503.78      | 503.99  | 503.56   |
| 5   | 1      | 508.86   | 508.78     | 508.83      | 508.82  | 508.44   |
| 5   | 2      | 610.100  | 608.51     | 610.09      | 610.12  | 609.24   |
| 5   | 3      | 610.38   | 608.75     | 610.32      | 610.35  | 609.47   |
| 5   | 4      | 742.10   | 731.51     | 742.10      | 742.10  | 740.54   |
| 5   | 5      | 742.11   | 731.52     | 742.10      | 742.11  | 740.55   |

Table 13 (Continued)

| $J$ | $\tau$ | Obs.    | Low $\tau$ | High $\tau$ | Low $J$ | High $J$ |
|-----|--------|---------|------------|-------------|---------|----------|
| 6   | -6     | 446.704 | 446.72     | 466.89      | 446.73  | 446.65   |
| 6   | -5     | 447.30  | 447.25     | 467.71      | 447.29  | 447.20   |
| 6   | -4     | 542.890 | 432.94     | 543.75      | 542.91  | 542.82   |
| 6   | -3     | 552.96  | 552.91     | 555.06      | 552.93  | 552.81   |
| 6   | -2     | 602.762 | 602.79     | 601.22      | 602.79  | 602.68   |
| 6   | -1     | 649.02  | 648.99     | 648.67      | 649.01  | 648.77   |
| 6   | 0      | 661.534 | 661.57     | 661.33      | 661.56  | 661.37   |
| 6   | 1      | 756.76  | 755.91     | 756.68      | 756.75  | 756.24   |
| 6   | 2      | 757.78  | 756.99     | 757.78      | 757.80  | 757.30   |
| 6   | 3      | 888.65  | 881.75     | 888.61      | 888.61  | 887.62   |
| 6   | 4      | 888.59  | 881.79     | 888.63      | 888.64  | 887.66   |
| 6   | 5      | 1045.11 | 1004.05    | 1045.08     | 1045.07 | 1043.59  |
| 6   | 6      | 1045.03 | 1004.05    | 1045.09     | 1045.07 | 1043.59  |
|     |        |         |            |             |         |          |
| 7   | -7     | 586.28  | 586.26     | 633.36      | 586.29  | 586.21   |
| 7   | -6     | 586.43  | 586.48     | 633.81      | 586.53  | 586.44   |
| 7   | -5     | 704.20  | 704.27     | 716.11      | 704.21  | 704.17   |
| 7   | -4     | 709.50  | 709.62     | 717.18      | 709.60  | 709.58   |
| 7   | -3     | 782.41  | 782.42     | 779.53      | 782.44  | 782.33   |
| 7   | -2     | 816.65  | 816.72     | 816.40      | 816.73  | 816.65   |
| 7   | -1     | 842.36  | 842.39     | 841.10      | 842.34  | 842.29   |
| 7   | 0      | 927.76  | 927.49     | 927.59      | 927.78  | 927.59   |
| 7   | 1      | 931.23  | 931.03     | 931.27      | 931.26  | 931.09   |
| 7   | 2      | 1059.68 | 1055.97    | 1059.67     | 1059.77 | 1059.19  |
| 7   | 3      | 1059.89 | 1056.18    | 1059.83     | 1059.96 | 1059.38  |
| 7   | 4      | 1216.39 | 1186.53    | 1216.24     | 1216.20 | 1215.33  |
| 7   | 5      | 1216.39 | 1186.54    | 1216.24     | 1216.21 | 1215.34  |
| 7   | 6      | 1394.85 | 1220.16    | 1394.85     | 1394.80 | 1393.83  |
| 7   | 7      | 1394.85 | 1220.16    | 1394.85     | 1394.80 | 1393.83  |
|     |        |         |            |             |         |          |
| 8   | -8     | 744.09  | 744.08     | 842.60      | 744.11  | 744.05   |
| 8   | -7     | 744.14  | 744.17     | 842.85      | 744.20  | 744.14   |
| 8   | -6     | 882.97  | 882.98     | 901.78      | 882.85  | 882.92   |
| 8   | -5     | 885.64  | 885.64     | 906.19      | 885.54  | 885.64   |
| 8   | -4     | 983.09  | 982.96     | 979.27      | 983.00  | 982.89   |
| 8   | -3     | 1006.14 | 1006.16    | 1006.68     | 1006.14 | 1006.18  |
| 8   | -2     | 1050.20 | 1050.18    | 1046.58     | 1050.14 | 1050.14  |
| 8   | -1     | 1122.78 | 1122.76    | 1122.14     | 1122.72 | 1122.80  |
| 8   | 0      | 1131.88 | 1131.89    | 1131.50     | 1131.77 | 1131.84  |
| 8   | 1      | 1255.19 | 1253.87    | 1255.21     | 1255.49 | 1255.14  |
| 8   | 2      | 1255.98 | 1254.65    | 1255.95     | 1256.25 | 1255.89  |
| 8   | 3,4    | 1411.59 | 1391.69    | 1411.66     | 1412.28 | 1411.30  |
| 8   | 5,6    | 1590.70 | 1445.84    | 1590.81     | 1590.78 | 1590.19  |

Table 13 (Continued)

| $J$ | $\tau$ | Obs.    | Low $\tau$ | High $\tau$ | Low $J$ | High $J$ |
|-----|--------|---------|------------|-------------|---------|----------|
| 8   | 7,8    | 1789.09 | 1068.80    | 1789.11     | 1789.76 | 1788.90  |
| 9   | -9     | 920.20  | 920.19     | 1110.24     | 920.16  | 920.18   |
| 9   | -8     | 920.22  | 920.23     | 1110.38     | 920.20  | 920.22   |
| 9   | -7     | 1079.16 | 1079.20    | 1125.76     | 1078.97 | 1079.19  |
| 9   | -6     | 1080.51 | 1080.49    | 1128.51     | 1080.23 | 1080.49  |
| 9   | -5     | 1202.04 | 1202.04    | 1200.51     | 1202.15 | 1202.00  |
| 9   | -4     | 1216.37 | 1216.31    | 1220.33     | 1216.27 | 1216.37  |
| 9   | -3     | 1283.02 | 1282.96    | 1275.59     | 1282.99 | 1282.93  |
| 9   | -2     | 1341.03 | 1341.06    | 1339.36     | 1340.89 | 1341.12  |
| 9   | -1     | 1360.56 | 1360.45    | 1358.43     | 1360.19 | 1360.37  |
| 9   | 0      | 1475.14 | 1475.11    | 1474.83     | 1475.54 | 1475.25  |
| 9   | 1      | 1477.46 | 1477.51    | 1477.38     | 1477.91 | 1477.55  |
| 9   | 2      | 1631.44 | 1618.68    | 1631.33     | 1633.23 | 1631.36  |
| 9   | 3      | 1631.58 | 1618.85    | 1631.14     | 1633.39 | 1631.50  |
| 9   | 4,5    | 1810.76 | 1691.12    | 1810.70     | 1813.20 | 1810.49  |
| 9   | 6,7    | 2009.99 | 1080.49    | 2010.05     | 2010.57 | 2009.79  |
| 9   | 8,9    | 2225.56 | -402.17    | 2225.6      | 2231.26 | 2226.16  |
| 10  | -10    | 1114.59 | 1114.59    | 1458.71     | 1114.40 | 1114.59  |
| 10  | -9     | 1114.59 | 1114.60    | 1458.79     | 1114.42 | 1114.60  |
| 10  | -8     | 1293.22 | 1293.17    | 1393.15     | 1292.81 | 1293.18  |
| 10  | -7     | 1293.80 | 1293.79    | 1394.85     | 1293.39 | 1293.78  |
| 10  | -6     | 1438.19 | 1438.15    | 1446.20     | 1438.49 | 1438.17  |
| 10  | -5     | 1446.23 | 1446.28    | 1460.28     | 1446.34 | 1446.29  |
| 10  | -4     | 1538.31 | 1538.28    | 1526.10     | 1538.54 | 1538.26  |
| 10  | -3     | 1581.53 | 1581.54    | 1578.48     | 1581.35 | 1581.60  |
| 10  | -2     | 1616.49 | 1616.6     | 1610.79     | 1616.51 | 1616.57  |
| 10  | -1     | 1719.36 | 1719.35    | 1717.66     | 1719.57 | 1719.11  |
| 10  | 0      | 1724.80 | 1725.42    | 1724.5      | 1725.67 | 1725.05  |
| 10  | 1      | 1875.24 | 1866.80    | 1875.06     | 1878.93 | 1875.34  |
| 10  | 2      | 1875.72 | 1867.38    | 1875.53     | 1879.49 | 1875.83  |
| 10  | 3,4    | 2054.55 | 1953.92    | 2054.44     | 2062.19 | 2054.55  |
| 10  | 5,6    | 2254.55 | 1663.37    | 2254.54     | 2262.43 | 2254.39  |
| 10  | 7,8    | 2471.59 | -4.64      | 2471.67     | 2475.64 | 2471.59  |
| 10  | 9,10   | 2702.09 | -5678.57   | 2702.21     | 2728.54 | 2702.83  |
| 11  | -10    | 1327.25 | 1327.23    | 1919.04     | 1326.76 | 1327.24  |
| 11  | -9     | 1525.02 | 1525.02    | 1720.42     | 1524.58 | 1525.02  |
| 11  | -8     | 1525.31 | 1525.33    | 1721.46     | 1524.83 | 1525.29  |
| 11  | -7     | 1690.85 | 1690.84    | 1722.93     | 1691.81 | 1690.92  |
| 11  | -6     | 1695.24 | 1695.27    | 1732.74     | 1695.85 | 1695.21  |
| 11  | -5     | 1813.47 | 1813.51    | 1797.41     | 1814.47 | 1813.54  |

Table 13 (Continued)

| $J$ | $\tau$ | Obs.    | Low $\tau$ | High $\tau$ | Low $J$ | High $J$ |
|-----|--------|---------|------------|-------------|---------|----------|
| 11  | -4     | 1843.32 | 1843.26    | 1839.63     | 1843.52 | 1843.24  |
| 11  | -3     | 1899.21 | 1899.17    | 1886.34     | 1899.61 | 1899.19  |
| 11  | -2     | 1968.08 | 1968.11    | 1982.30     | 1987.22 | 1986.14  |
| 11  | -1     | 1999.34 | 1999.31    | 1997.22     | 2000.58 | 1999.26  |
| 11  | 0      | 2143.01 | 2135.5     | 2142.30     | 2149.28 | 2143.04  |
| 11  | 1      | 2144.46 | 2137.18    | 2144.11     | 2150.90 | 2144.48  |
| 11  | 2      | 2322.20 | 2232.40    | 2321.9      | 2337.89 | 2322.18  |
| 11  | 3      | 2322.25 | 2232.59    | 2322.93     | 2338.80 | 2322.27  |
| 11  | 4,5    | 2522.46 | 1975.18    | 2522.45     | 2536.28 | 2522.50  |
| 11  | 6,7    | 2740.73 | 391.39     | 2740.90     | 2762.64 | 2740.64  |
| 11  | 8,9    | 2973.07 | -5100.52   | 2973.43     | 2991.54 | 2973.13  |
| 11  | 10,11  | 3216.6  | -20510.2   | 3216.74     | 3309.34 | 3216.59  |
| 12  | -11    | 1558.07 | 1558.10    | 2632.95     | 1557.10 | 1558.07  |
| 12  | -10    | 1774.75 | 1774.75    | 2131.17     | 1774.45 | 1774.75  |
| 12  | -9     | 1774.88 | 1774.91    | 2131.77     | 1774.56 | 1774.86  |
| 12  | -8     | 1960.38 | 1960.25    | 2041.81     | 1962.71 | 1960.40  |
| 12  | -7     | 1962.60 | 1962.66    | 2048.45     | 1964.66 | 1962.55  |
| 12  | -6     | 2106.7  | 2106.30    | 2091.60     | 2109.04 | 2166.43  |
| 12  | -5     | 2124.84 | 2125.26    | 2125.03     | 2126.98 | 2125.05  |
| 12  | -4     | 2205.95 | 2205.80    | 2182.65     | 2207.84 | 2206.12  |
| 12  | -3     | 2275.65 | 2274.84    | 2267.23     | 2278.29 | 2275.60  |
| 12  | -2     | 2300.94 | 2299.92    | 2294.21     | 2303.62 | 2300.89  |
| 12  | -1     | 2434.14 | 2424.51    | 2431.84     | 2444.38 | 2434.17  |
| 12  | 0      | 2437.84 | 2428.58    | 2437.32     | 2448.32 | 2437.84  |
| 12  | 1      | 2613.26 | 2525.07    | 2612.72     | 2640.55 | 2613.22  |
| 12  | 2      | 2613.49 | 2525.69    | 2613.04     | 2640.98 | 2613.52  |
| 12  | 3,4    | 2813.94 | 2290.85    | 2813.58     | 2863.07 | 2813.94  |
| 12  | 5,6    | 3033.17 | 776.45     | 3033.08     | 3095.21 | 3033.15  |
| 12  | 7,8    | 3267.2  | -4552.03   | 3267.49     | 3322.66 | 3267.23  |
| 12  | 9,10   | 3512.8  | -19625.6   | 3513.24     | 3577.09 | 3512.78  |
| 12  | 11,12  | 3767.1  | -57005.3   | 3767.35     | 4039.92 | 3767.11  |
| 13  | -12    | 1806.94 | 1807.12    | 3355.04     | 1805.35 | 1807.07  |
| 13  | -11    | 2042.5  | 2042.29    | 2657.93     | 2042.62 | 2042.32  |
| 13  | -10    | 2042.5  | 2042.38    | 2658.27     | 2042.67 | 2042.37  |
| 13  | -9     | 2247.0  | 2246.61    | 2419.79     | 2252.17 | 2246.86  |
| 13  | -8     | 2248.24 | 2247.97    | 2424.12     | 2253.06 | 2247.89  |
| 13  | -7     | 2415.95 | 2415.15    | 2515.60     | 2421.83 | 2415.30  |
| 13  | -6     | 2426.0  | 2426.62    | 2440.29     | 2431.94 | 2426.14  |
| 13  | -5     | 2534.14 | 2533.83    | 2498.00     | 2539.84 | 2534.87  |
| 13  | -4     | 2586.5  | 2584.84    | 2571.60     | 2593.10 | 2586.63  |
| 13  | -3     | 2629.54 | 2626.94    | 2613.01     | 2635.38 | 2629.86  |



Table 13 (Continued)

| $J$ | $\tau$  | Obs.    | Low $\tau$ | High $\tau$ | Low $J$ | High $J$ |
|-----|---------|---------|------------|-------------|---------|----------|
| 13  | -2      | 2748.4  | 2733.45    | 2741.74     | 2764.80 | 2748.86  |
| 13  | -1      | 2756.61 | 2742.40    | 2755.00     | 2772.98 | 2756.64  |
| 13  | 0       | 2927.38 | 2830.87    | 2926.10     | 2970.87 | 2927.54  |
| 13  | 1       | 2928.45 | 2832.61    | 2927.60     | 2971.94 | 2928.39  |
| 13  | 2,3     | 3128.25 | 2606.58    | 3127.55     | 3214.14 | 3128.63  |
| 13  | 4,5     | 3348.2  | 1141.36    | 3347.83     | 3476.44 | 3348.99  |
| 13  | 6,7     | 3584.0  | -4051.36   | 3583.93     | 3729.26 | 3585.09  |
| 14  | -13     | 2073.81 | 2074.26    | 4455.38     | 2071.36 | 2074.18  |
| 14  | -12,-11 | 2328.2  | 2327.55    | 3344.54     | 2329.42 | 2327.71  |
| 14  | -10     | 2551.0  | 2550.00    | 2881.32     | 2561.44 | 2550.48  |
| 14  | -9      | 2551.5  | 2550.81    | 2884.04     | 2561.83 | 2550.95  |
| 14  | -8      | 2740.5  | 2739.75    | 2777.00     | 2754.14 | 2739.99  |
| 14  | -7      | 2745.5  | 2746.62    | 2795.93     | 2759.37 | 2745.77  |
| 14  | -6      | 2883.5  | 2880.40    | 2833.20     | 2895.31 | 2882.81  |
| 14  | -5      | 2919.5  | 2915.40    | 2896.48     | 2932.91 | 2918.34  |
| 14  | -4      | 2983.6  | 2978.52    | 2950.65     | 2996.26 | 2984.97  |
| 14  | -3      | 3085.0  | 3062.08    | 2069.50     | 3112.04 | 2085.14  |
| 14  | -2      | 2101.65 | 3079.68    | 3095.90     | 3126.69 | 2101.92  |
| 14  | -1      | 3264.2  | 3149.09    | 3260.45     | 3330.35 | 3265.01  |
| 14  | 0       | 3266.36 | 3153.50    | 3265.55     | 3332.42 | 3267.16  |
| 14  | 1       | 3465.18 | 2919.25    | 3463.73     | 3601.09 | 3466.33  |
| 14  | 2       | 3465.4  | 2920.39    | 3464.02     | 3601.39 | 2466.51  |
| 15  | -14     | 2358.58 | 2359.48    | 5922.20     | 2355.02 | 2359.39  |
| 15  | -13,-12 | 2631.6  | 2630.24    | 4247.55     | 2635.20 | 2630.78  |
| 15  | -11     | 2872.56 | 2870.39    | 3460.38     | 2892.11 | 2871.31  |
| 15  | -10     | 2872.9  | 2870.89    | 3462.01     | 2892.28 | 2871.52  |
| 15  | -9      | 3081.2  | 3080.57    | 3195.62     | 3108.79 | 3080.44  |
| 15  | -8      | 3084.2  | 3084.83    | 3208.91     | 3111.28 | 3083.37  |
| 15  | -7      | 3252.0  | 3243.24    | 3193.34     | 3275.73 | 3247.56  |
| 15  | -6      | 3277.0  | 3265.96    | 3246.43     | 3300.36 | 3269.89  |
| 15  | -5      | 3365.0  | 3351.38    | 3304.39     | 3387.88 | 3364.21  |
| 15  | -4      | 3446.0  | 3410.08    | 3412.86     | 3489.23 | 3444.01  |
| 15  | -3      | 3473.0  | 3440.70    | 3456.91     | 3512.13 | 3474.67  |
| 15  | -2      | 3624.0  | 3479.27    | 3613.14     | 3722.01 | 3625.56  |
| 15  | -1      | 3628.7  | 3489.49    | 3626.89     | 3724.61 | 3630.45  |
| 15  | 0       | 3824.8  | 3226.47    | 3820.93     | 4027.40 | 3827.28  |
| 15  | 1       | 3862.1  | 3229.82    | 3822.42     | 4027.86 | 3827.75  |
| 15  | 2,3     | 4045.8  | 1778.31    | 4042.73     | 4400.08 | 4050.58  |
| 16  | -16,-15 | 2661.2  | 2662.73    | 7864.79     | 2656.20 | 2662.68  |
| 16  | -14,-13 | 2953.0  | 2950.21    | 5440.64     | 2960.64 | 2951.52  |

Table 13 (Continued)

| <u>J</u> | <u><math>\tau</math></u> | <u>Obs.</u> | <u>Low <math>\tau</math></u> | <u>High <math>\tau</math></u> | <u>Low J</u> | <u>High J</u> |
|----------|--------------------------|-------------|------------------------------|-------------------------------|--------------|---------------|
| 16       | -12, -11                 | 3211.5      | 3207.66                      | 4202.60                       | 3246.26      | 2662.68       |
| 16       | -10                      | 3437.7      | 3438.43                      | 3695.47                       | 3489.79      | 3437.12       |
| 16       | -9                       | 3439.7      | 3441.21                      | 3704.34                       | 3490.89      | 3438.54       |
| 16       | -8                       | 3640.3      | 3621.81                      | 3588.72                       | 3685.03      | 3627.63       |
| 16       | -7                       | 3657.1      | 3636.46                      | 3631.32                       | 3699.97      | 3640.54       |

#### High $\tau$

Next, examine the high  $\tau$  fit. An examination of table 13 shows that deviations of a few wave numbers arise for low  $J_\tau$  levels, such as 4<sub>-4</sub>, 4<sub>-3</sub>, 5<sub>-5</sub>, 5<sub>-4</sub>. For 6<sub>-6</sub>, 6<sub>-5</sub>, it is  $\sim 20 \text{ cm}^{-1}$ , and this trend continues (getting worse) for all the low  $\tau$  states, e.g., for 10<sub>-10</sub>, it is over 300 wave numbers. These difficulties arise from and reflect the strong rotation-vibration correlations that exist for high  $\tau$  levels, which in turn manifest themselves in the various coefficients.

#### Low $J$

The Hamiltonian was chosen so that the  $J = 1$  through 8 states were fit to  $\sim 0.05 \text{ cm}^{-1}$ . An examination of table 13 reveals that difficulties manifest themselves almost immediately. For example, in the 9<sub>2</sub> state, there is a deviation of  $2 \text{ cm}^{-1}$ ; and by 9<sub>9</sub>, it is  $6 \text{ cm}^{-1}$ . The situation continues to worsen, e.g., 10<sub>1</sub> is off by  $2 \text{ cm}^{-1}$ , 10<sub>10</sub> by  $26 \text{ cm}^{-1}$ . For  $J = 1$ , difficulties arise by 11<sub>-2</sub> ( $1 \text{ cm}^{-1}$ ); and by 11<sub>11</sub>, it is  $100 \text{ cm}^{-1}$ . Thus, the ability of this fit to predict high states is virtually nonexistent.

#### High $J$

The  $J = 10, 11$ , and 12 levels were fit. With few exceptions, all of the states were fit to better than  $0.05 \text{ cm}^{-1}$ . The pattern is very similar to the situation that arose for the rotating Morse oscillator when the levels  $J = 10$  to 20 were fit; namely, the low-lying levels are reasonably well predicted. However, there was immediate difficulty for the higher states, i.e., 13<sub>6</sub> deviated by  $1 \text{ cm}^{-1}$ , 14<sub>3</sub> by  $3 \text{ cm}^{-1}$ , 15<sub>8</sub> by  $3 \text{ cm}^{-1}$ , 15<sub>3</sub> by  $5 \text{ cm}^{-1}$ , 16<sub>-8</sub> by  $13 \text{ cm}^{-1}$  and 16<sub>-7</sub> by  $17 \text{ cm}^{-1}$ .

#### Microwave Spectral Data

This work (ref. 1) is a spectroscopic fit to the spectral data that arise from microwave transitions between the low energy rotational states through  $J = 10$ . The results of predictions for this case are qualitatively similar, although quantitatively superior to the predictions of the other fits. An examination of tables 9 and 10 reveals the following features. All of the rotational levels through 8<sub>8</sub> are predicted

to within a few hundredths of a wave number. Beyond this, more serious difficulties arise. For example, for the  $9_2$  through  $9_9$  levels, deviations on the order of a few tenths of a wave number arise between the predicted levels and the measured ones. Furthermore, some of the high  $\tau$  states of the  $J = 10$  multiplet are off by almost half of a wave number. For the remaining levels, a pattern that is similar to that for high and low  $\tau$ , as well as for high and low  $J$  appears, although this case is quantitatively more accurate. Within the  $J = 11$  series, deviations on the order of several wave numbers arise; and for the  $12_{11}$  and  $12_{12}$  states (where  $E_{10} > 100 \text{ cm}^{-1}$ ), discrepancies of over  $30 \text{ cm}^{-1}$  appear. At the moment, enough data are not available beyond the  $J = 12$  states to thoroughly examine further predictions of the microwave fit. However, it is undoubtedly safe to assume that deviations continue to increase and, in addition, that they appear for lower  $\tau$  numbers as  $J$  increases.



## SECTION VI

### DISCUSSION AND CONCLUSIONS

In this paper we have examined the usefulness and reliability of power series expansion techniques (as embodied in Watson's rotational Hamiltonian) in elucidating the rotational structure of light asymmetric highly anharmonic molecules, particularly water. This question has been examined within the framework of both a model system (i.e., the rotating Morse oscillator) as well as in the water molecule itself. In particular, for water, the Hamiltonian has terms of order  $P^{10}$  and involves 18 perturbation coefficients in addition to the three rotational constants. In both cases, the expansion techniques proved useful only for the low-lying rotational levels. For such states, the rotation-vibration interaction is relatively weak, and a power series expansion based on the picture of a slightly deformed rotor is valid. This is borne out by the rapid convergence of the various perturbation terms displayed in table 9. Similar behavior was exhibited by the rotating Morse oscillator. On the other hand, in attempts to apply the same procedure to the high-lying rotational states, serious difficulties immediately appeared. For those states, the molecular rotation velocity is large, and both the centripetal and coriolis (for polyatomic molecules) forces are large and, in turn, deform the molecule in a significant manner. Since these deformations represent huge perturbations away from the rigid rotor structure, many rotation-distortion terms are required to correctly describe the physical state of the molecule. To date, calculations are limited to tenth-order perturbations (i.e.,  $P^{10}$  terms), and the convergence results exhibited in tables 9 and 10 show that this is not enough, i.e.,  $P^{12}$ ,  $P^{14}$ , etc., type terms are required. The type of difficulties that arise depends on the data used to determine the various rotation and rotation-distortion coefficients. Thus, data that arise from the low-lying levels cannot be used to accurately predict the level structure for the higher states. In addition, although the first few rotation-distortion coefficients are accurately

determined, the higher-order ones may not be. This is due to the fact that the low-lying levels are only weakly deformed from the rigid rotor structure and, consequently, are not a sensitive measure of  $P^8$  and  $P^{10}$  type terms. Evidence of this behavior appears in tables 10 and 13. Attempts to circumvent these problems by fitting to higher rotational levels results in a new host of difficulties. In particular, the rotational constants deviate considerably from their expected values, and this gives rise to an incorrect picture of the geometric structure of the molecules. In addition, it also appears that one cannot predict the rotation energies of the low-lying levels (see table 13) for  $H_2O$ , which implies that all of the lower-order rotation distortion coefficients are in serious error. This is clearly brought out in tables 11 and 12. In the case of the rotating Morse oscillator, the low-lying level structures were predicted reasonably accurately, although the various rotation and rotation-distortion coefficients were in strong disagreement with the low energy fit. The physical basis for these difficulties lies in the fact that in attempts to fit the distortion constants to the high-lying levels, higher-order rotation-vibration correlations (i.e., 12th etc.) are folded into the lower order coefficients. As a consequence, the rotational wave functions will bear little resemblance to reality.

Another difficulty that arises is due to the large number of perturbation coefficients and the limited amount of convergent levels to fit these coefficients. This causes many of the coefficients that are determined in a least squares manner to be highly correlated. In turn, serious doubts are cast as to whether or not these numbers really represent the physical quantities that they should. A related problem arises in trying to include higher order distortion effects, i.e.,  $P^{12}$ ,  $P^{14}$ , ... terms in the Watson Hamiltonian. In particular, there are many more unknown coefficients to determine and only a limited number of energy levels. Although there are far more spectral lines than energy levels, these lines contain no more information on the structure of the molecule than do the rotational energies. Hence,

although there are more data points to fit, they are highly correlated; this, in turn, gives rise to strong correlations among the higher order coefficients thus reducing their reliability.

Another feature that should be pointed out is that the rotation constants depend on the energy denominators  $(E_{VJ\tau} - E_{V',J',\tau'})$ , which can be replaced by  $(E_{VJ} - E_{V',J'})$  only for the low-lying states. For higher energy levels, the rotational splitting can be on the order of the vibrational spacing. The rotation and rotation-distortion constants then depend sensitively on the particular rotational states used for fitting purposes, and these will not be unique, i.e., they will vary with the set of levels used as input data. This is clearly displayed in tables 7, 11, and 12.

Therefore, although this approach will work for low energy rotational levels, it does not work and, on the theoretical grounds just mentioned, cannot work for higher  $J$  or high  $\tau$  states. If reliable wave functions need to be obtained for the higher rotational states ( $J \geq 10$ ) in addition to the lower ones, another approach would be required. Finally, in order to obtain the rotational level structure in a different vibrational band, the entire process would have to be repeated since the various rotation and rotation-distortion coefficients will vary significantly with the vibrational state of the molecule.

# APPENDIX

## THE EFFECTS OF MATRIX DIAGONALIZATION ON THE DISTORTION ENERGIES

In this appendix we examine the effects of matrix diagonalization on the various rotational distortion energies, i.e.,  $E_4$ ,  $E_6$ , etc. For convenience, decompose the rotational Hamiltonian into a rigid rotor piece  $\mathcal{H}_0$  plus a distortion term  $\mathcal{H}'$  where

$$\mathcal{H}' = \mathcal{H}_4 + \mathcal{H}_6 + \mathcal{H}_8 + \mathcal{H}_{10} \quad (A1)$$

In equation (A1),  $\mathcal{H}_4$ ,  $\mathcal{H}_6$ , ... refer to the fourth, sixth, ... order distortion terms.

Note that the results of table 9 show that effects of matrix diagonalization on the total energy are small, which justifies using perturbation theory in the analysis given below. The leading correction to the rotational eigenvector due to  $\mathcal{H}'$  is

$$|J_\tau\rangle_{M.D.} = |J_\tau\rangle + \sum_{\tau'} \frac{\langle J_{\tau'} | \mathcal{H}' | J_\tau \rangle}{(E_{J_{\tau'}} - E_{J_\tau})} |J_{\tau'}\rangle \quad (A2)$$

In equation (A2),  $|J_\tau\rangle_{M.D.}$  refers to the matrix diagonalized eigenvector and  $|J_\tau\rangle$  to the rigid-rotor eigenvector. The effects of matrix diagonalization, for any distortion term, say the fourth,

$$\begin{aligned} \delta E_{J_\tau}^{(4)} &\equiv_{M.D.} \langle J_\tau | \mathcal{H}_4 | J_\tau \rangle_{M.D.} - \langle J_\tau | \mathcal{H}_4 | J_\tau \rangle \\ &\approx 2 \sum_{\tau'} \left\{ \frac{\langle J_\tau | \mathcal{H}_4 | J_{\tau'} \rangle \langle J_{\tau'} | \mathcal{H}' | J_\tau \rangle}{(E_{J_{\tau'}} - E_{J_\tau})} \right\} \quad (A3) \end{aligned}$$

To estimate the size of these terms, note that the perturbing Hamiltonian has all the symmetries  $\mathcal{H}_0$ ; consequently, it will connect the state  $J_\tau$  only to those states  $J_{\tau'}$ , such that



$$\tau' = \tau \pm 4n; \quad n = 1, 2, \dots, \quad (\text{A4})$$

Now, due to the large spacings between those different states that are connected by  $\mathcal{H}'$  it follows that the major contributions (A2) and (A3) arise from the  $n = 1$  term. As a specific example, we consider the  $10_{10}$  state. Then, the dominant contribution arises from the  $10_6$  state and since from the definition of  $\Delta E$

$$\begin{aligned} \Delta E &= \sum_n \delta E_n \\ n &= 4 \end{aligned} \quad (\text{A5})$$

so that for  $10_{10}$ ,

$$0.03 \text{ cm}^{-1} = \frac{|\langle 10_{10} | \mathcal{H}' | 10_6 \rangle|^2}{600} \quad (\text{A6})$$

from which it follows that

$$|\langle 10_{10} | \mathcal{H}' | 10_6 \rangle| \approx 5 \text{ cm}^{-1}$$

To evaluate the leading contributions to  $\delta E^{(4)}$ ,... in general, expect

$$\langle J_\tau | \mathcal{H}_n | J_\tau \rangle > \langle J_\tau + 4 | \mathcal{H}_n | J_\tau \rangle. \quad (\text{A7})$$

Thus,

$$\delta E_n(10_{10}) \leq \frac{5}{600} E_n \lesssim 10^{-2} E_n \quad (\text{A8})$$

and the various corrections are

$$|\delta E^{(4)}| \lesssim 2.76 \text{ cm}^{-1}$$

$$|\delta E^{(6)}| \lesssim 0.11 \text{ cm}^{-1}$$

$$|\delta E^{(8)}| \lesssim 0.05 \text{ cm}^{-1}$$

$$|\delta E^{(10)}| \lesssim 0.02 \text{ cm}^{-1}.$$

## REFERENCES

1. De Lucia, F., Helminger, P., Cook, R., and Gordy, W., "Submillimeter Microwave Spectrum of  $\text{H}_2^{16}\text{O}$ ," Phys. Rev. A5, 487, 1972.
2. De Lucia, F., Helminger, P., Gordy, W., Morgan, H., and Staats, P., "Microwave Rotation-Inversion Spectrum of  $\text{NT}_3$ ," Phys. Rev. A9, 12, 1974.
3. Pugh, L., and Rao, K., "Spectrum of Water Vapor in 1.9 and 2.7  $\mu$  Regions," J. Mol. Spectrosc. 47, 403, 1973.
4. Fraley, P. E., and Rao, K., "High Resolution Infrared Spectra of Water Vapor  $\nu_1$  and  $\nu_3$  Bands of  $\text{H}_2^{16}\text{O}$ ," J. Mol. Spectrosc. 29, 348, 1969.
5. Rogovin, D., Sargent, M., and Tigelaar, H., "A Simple, Reliable Model of the Bending Mode of Water," Chem. Phys. Letts. 31, 147, 1975.
6. Izatt, J. R., Sakai, H., and Benedict, W. S., "Positions, Intensities, and Widths of Water-Vapor Lines between 475 and 692  $\text{cm}^{-1}$ ," J. Opt. Soc. Am. 59, 19, 1969.
7. Winton, R. S., and Gordy, W., "High-Precision Millimeter-Wave Spectroscopy with the Lamb Dip," Phys. Letts. 32A, 219, 1970.
8. Hougen, J. T., Bunker, P. R., and Johns, J. W. C., "The Vibration-Rotation Problem in Triatomic Molecules Allowing for a Large Amplitude Bending Vibration," J. Mol. Spectrosc. 34, 136, 1970.
9. Bunker, P. R., and Stone, J. M. R., "The Bending Rotation Hamiltonian for the Triatomic Molecule and Application to HCN and  $\text{H}_2\text{O}$ ," J. Mol. Spectrosc. 41, 310, 1972.
10. "Absorption of Infrared Laser Radiation in the Atmosphere," Proceedings of Mitre Meeting, April 1973, published by Mitre Corp., Bedford, Massachusetts.
11. Watson, K. G., "Centrifugal Correction for Asymmetric Top Molecules," J. Chem. Phys. 45, 1360, 1966.
12. Born, M., and Oppenheimer, J. R., "Zur Quantentheorie der Molekelin," Ann. Physik 84, 457, 1927.
13. Franks, Felix, ed., Water A Comprehensive Treatise, Vol. 2, Plenum Press, N.Y., 1972.

14. Howard, J. B., and Wilson, E. B., "Normal Frequencies of Vibration of Symmetrical Pyramidal Molecules  $AB_3$  with Application to the Raman Spectra of Trihalides," J. Chem. Phys. 2, 630, 1934.
15. Bendick, W. S., Clough, S. A., Frenkel, L., and Sullivan, T. E., "Microwave Spectrum and Rotational Constants for the Ground States of  $D_2O$ ," J. Chem. Phys. 53, 2565, 1970.
16. Pekeris, C. L., "The Rotation-Vibration Coupling in Diatomic Molecules," Phys. Rev. 45, 98, 1934.
17. Dennison, D. M., and Hecht, K. T., Aggregates of Particles, Molecular Spectra, in the series Quantum Theory II, D. R. Bates, ed., Academic Press, New York, 1961.
18. Hall, R. T., and Dowling, J. M., "Pure Rotational Spectrum of Water Vapor," J. Chem. Phys. 47, 2454, 1967.